



Contents lists available at [SciVerse ScienceDirect](http://SciVerse.ScienceDirect)

European Journal of Cell Biology

journal homepage: www.elsevier.de/ejcb



Role for CD74 and CXCR4 in clathrin-dependent endocytosis of the cytokine MIF

Verena Schwartz^a, Alexander Krüttgen^{b,1}, Joachim Weis^b, Christian Weber^c,
Tammo Ostendorf^d, Hongqi Lue^a, Jürgen Bernhagen^{a,*}

^a Institute of Biochemistry and Molecular Cell Biology, RWTH Aachen University, Pauwelsstraße 30, D-52074 Aachen, Germany

^b Institute of Neuropathology, RWTH Aachen University, Pauwelsstraße 30, D-52074 Aachen, Germany

^c Institute for Cardiovascular Prevention, Ludwig-Maximilians-Universität Munich, Pettenkoferstraße 8a und 9, 80336 Munich, Germany

^d Medical Department II, RWTH Aachen University, Pauwelsstraße 30, D-52074 Aachen, Germany

ARTICLE INFO

Article history:

Received 23 May 2011

Received in revised form 2 August 2011

Accepted 28 August 2011

Keywords:

Cytokine

Chemokine

G protein-coupled receptor (GPCR)

Uptake

MIF receptor

Endosomal signaling

Dynamin

β-Arrestin

Heteromeric receptor complex

Inflammation

ABSTRACT

Macrophage migration inhibitory factor (MIF) is a pleiotropic cytokine that plays a role in innate and adaptive immunity. Depending on the cellular context and disease state, MIF signaling is mediated by its receptors CXCR2, CXCR4 and/or CD74. Although it is known that MIF is endocytosed, the exact mechanism has remained unknown. In exploring the mechanism of MIF endocytosis with biologically active Alexa⁵⁴⁶MIF, pathway-specific inhibitors (monodansylcadaverine, MDC; chlorpromazine, CPZ; dynasore; dominant-negative dynamin, bafilomycin, nocodazole) and receptor overexpression and blockade approaches, we identified a clathrin/dynamin-dependent endocytosis pathway as the main track for MIF internalization. MIF endocytosis was rapid and colocalization with both early and late endosomal vesicles in a microtubule- and acidification-dependent manner was observed. LDL endocytosis (which is clathrin-mediated) served as a control and was similarly inhibited by MDC or dynasore. When MIF endocytosis was compared to that of transferrin, acetylated LDL, and cholera toxin B (the latter internalized by a clathrin-independent pathway) by colocalization studies, the MIF internalization pathway clearly resembled that of LDL but also shared early trafficking with transferrin, whereas no colocalization with cholera toxin was noted. To identify the receptors involved in MIF endocytosis, we focused on CD74 and CXCR4 which form a heteromeric complex. Ectopic overexpression of CD74 in HEK293 and HeLa cells, which do not endogenously express CD74, led to a marked acceleration of MIF endocytosis while pharmacological blockade of CXCR4, which is endogenously expressed on these cells, with AMD3100 led to a 20% reduction of MIF endocytosis in HEK293-CD74 transfectants, whereas in untransfected cells, a blockade of 40% was observed. Of note, both CD74 and CXCR4 strongly colocalize with Alexa⁵⁴⁶MIF both on the plasma membrane and in endosomal compartments. Moreover, MIF-stimulated AKT signaling, which was previously shown to involve both CD74 and CXCR4, was reduced by endocytosis inhibitors, indicating that MIF signaling is at least in part due to endosomal signaling mechanisms. Thus, MIF uptake follows a rapid LDL-like, clathrin- and dynamin-dependent endocytosis pathway, which is dependent on the receptors CD74 and CXCR4 and leads to the initiation of endosomal signaling responses.

© 2011 Elsevier GmbH. All rights reserved.

Introduction

In mammals, protein endocytosis may occur by one of three possible pathways: (i) clathrin-dependent internalization, (ii) clathrin-independent internalization through caveolae/lipid rafts, and (iii) clathrin- and caveolin-independent internalization (Gould and Lippincott-Schwartz, 2009). For all three pathways, prominent representatives are known. Transferrin, low-density lipoprotein

(LDL) and epidermal growth factor (EGF) (Carpenter and Cohen, 1979; Ghosh et al., 1994; Goldstein et al., 1979, 1985; Wall et al., 1980) are proteins that internalize via the clathrin-associated pathway, whereas toxins, viruses and bacterial proteins are known to be endocytosed by clathrin-independent pathways. Lastly, integrins, MHC complex molecules, and glycosylphosphatidylinositol (GPI)-anchored proteins are internalized via clathrin- and caveolin-independent pathways (Gould and Lippincott-Schwartz, 2009). Cholera toxin B is a good marker for the caveolin-mediated endocytosis pathway, as it clusters in caveolae, although it is not exclusively endocytosed via this track (Montesano et al., 1982; Tran et al., 1987). Both the clathrin-dependent and the clathrin-independent, caveolin-dependent endocytosis pathways need the GTPase dynamin for vesicle budding-off from the plasma

* Corresponding author. Tel.: +49 241 80 88840; fax: +49 241 80 82427.

E-mail address: jbernhagen@ukaachen.de (J. Bernhagen).

¹ Present address: Dr. Stein + Kollegen, Wallstraße 10, 41061 Mönchengladbach, Germany.

membrane, whereas the clathrin- and caveolin-independent internalization pathway requires the action of the GTPase ARF6 (Gould and Lippincott-Schwartz, 2009; Marchese et al., 2003). Sorting of internalized ligands and receptors to different destinations in the cell is believed to be the primary function of the endocytic system. In addition, further functions for endosomes, e.g. in signaling, cytokinesis, polarity, and cell migration have been recognized (Gould and Lippincott-Schwartz, 2009; Lakadamyali et al., 2006; Miaczynska and Bar-Sagi, 2010; Miaczynska et al., 2004). This work also has led to the concept of 'signaling endosomes' (Sorkin and von Zastrow, 2002; von Zastrow and Sorkin, 2007). Lakadamyali et al. showed that early endosomes consist of two distinct populations which differ in their maturation time to late endosomes. They named them a dynamic population which is highly mobile on microtubules and rapidly matures towards late endosomes and a static population with a slow maturation time (Lakadamyali et al., 2006). Transferrin, LDL, and EGF which we used as controls and reference proteins in the present investigation, are believed to first enter a common pool of early endosomes prior to sorting to recycling or late endosomes (Dickson et al., 1983; Dunn et al., 1989; Ghosh et al., 1994). The GTPases Rab5 and Rab7 are markers for early and late endosomes, respectively, but some portion of Rab7 also is detected on early endosomes while some Rab5 also traffics on to the late endosome.

Cytokines are important multifunctional mediators which broadly modulate innate and adaptive immunity responses by target cell-specific receptor-mediated pathways. Endocytosis of cytokine/cytokine receptor complexes occurs rapidly upon cytokine ligation and serves to switch-off the elicited cellular response (Thomson, 2003). It has also been established that cytokine signaling can be specifically induced after endocytosis of the ligand/receptor complex, thus constituting cytokine-induced endosomal signaling (Gould and Lippincott-Schwartz, 2009).

Macrophage migration inhibitory factor (MIF) was originally discovered as a lymphocyte mediator which inhibits the random migration of macrophages. Today, it is clear that MIF is a pleiotropic inflammatory cytokine that regulates a broad range of immune and inflammatory activities. MIF is a critical upstream regulator of innate immunity, which e.g. upregulates Toll-like receptor 4 (TLR4) expression in monocytes/macrophages. Dysregulated MIF functions have been recognized to critically contribute to a number of acute and chronic inflammatory diseases such as septic shock, rheumatoid arthritis, glomerulonephritis, colitis, Crohn's disease, and atherosclerosis, as well as tumorigenesis. MIF is expressed in a wide range of tissues and cell types. In contrast, its secretion, which occurs by a non-classical pathway, is specifically triggered by inflammatory and redox stress stimuli and mainly occurs from monocytes/macrophages, endothelial cells, T cells as well as selective parenchymal cell types (Calandra and Roger, 2003).

Three receptors have been identified for MIF of which one solely interacts with MIF whereas the two other ones have more promiscuous binding features. The cell surface-expressed form of CD74/li, a single-pass type II membrane protein also known as the invariant chain (li) of the major histocompatibility factor class II (MHC II) and MHC II chaperone (Borghese and Clanchy, 2011; Busch et al., 2005; Stern et al., 2006) was identified as a high affinity MIF receptor on class II-positive cells including monocytes/macrophages and B lymphocytes (Leng et al., 2003; Matza et al., 2003). However, CD74/li may be upregulated under inflammatory conditions on class II-negative cells including endothelial cells and certain tumor cells, on which it also serves to mediate MIF activities (Borghese and Clanchy, 2011; Matza et al., 2003). The MIF/CD74 axis has been found to stimulate rapid and sustained ERK1/2 signaling, PI3K/AKT signaling, cell proliferation, and anti-apoptotic functions of MIF (Binsky et al., 2007; Lue et al., 2006, 2007; Meyer-Siegler et al., 2006; Shi et al., 2006). MIF also is a

non-cognate, high affinity ligand for the chemokine receptors CXCR2 and CXCR4 (Bernhagen et al., 2007; Cho et al., 2010; Vera et al., 2008); however, in the present study we are focusing on the CXCR4 subtype of MIF's chemokine receptors only. CXCR4 belongs to the large family of seven helix membrane-spanning G protein-coupled receptors. The *bona fide* ligand of CXCR4 is stromal-derived factor-1 α (SDF-1 α /CXCL-12) (Moser and Loetscher, 2001; Murphy et al., 2000; Rot and von Andrian, 2004; Thelen and Stein, 2008; Weber et al., 2004). By activating CXCR4, MIF promotes T-cell chemotaxis and integrin-dependent arrest on atherogenic endothelial surfaces. Accordingly, numerous *in vivo* studies in pro-atherogenic mouse models have demonstrated that the MIF/CXCR4 axis critically contributes to atherogenic leukocyte recruitment and atheroprogession (Bernhagen et al., 2007; Burger-Kentischer et al., 2002; Schober et al., 2004; Zerneck et al., 2008). The MIF/CXCR4 axis also regulates endothelial progenitor cell migration and cancer cell metastasis (Dessein et al., 2010; Simons et al., 2011; Tarnowski et al., 2010). Of note, CD74 can engage in heteromeric receptor complexes with CXCR4 (Bernhagen et al., 2007; Schwartz et al., 2009), although it is currently unknown whether CD74 and CXCR4 are part of a larger signaling complex or interact directly and bilaterally (Noels et al., 2009).

MIF endocytosis pathways were first studied in the context of experiments that demonstrated that intracellular, cytosolic, MIF interacts with the COP9 signalosome (CSN) component JAB1/CSN5. Exogenous MIF added to macrophages interacts with CSN5 following cellular uptake and cytosolic translocation from the endo-/lysosomal pathway (Kleemann et al., 2000, 2002). In these initial studies, MIF endocytosis was thought to occur by a receptor-independent mechanism. Later studies indicated that the cellular uptake of MIF can occur in a rapid manner at physiological MIF concentrations, implying that it may follow a canonical receptor-mediated endocytosis pathway (Berndt et al., 2008; Lue et al., 2006). However, it remained unknown which of the established endocytic pathways known in mammals MIF uptake follows and which exact mechanism is involved. Mechanistic aspects of the MIF endocytosis pathway have not become apparent until very recently, when it was suggested that MIF endocytosis involves β -arrestin-1 and CD74, and is promoted by complex formation with thioredoxin (TRX) (Son et al., 2009; Xie et al., 2011).

Here we sought to characterize the molecular features of the endocytosis pathway of MIF. Applying biologically active, fluorescently labeled Alexa⁵⁴⁶MIF, early and late endosomal colocalization experiments, confocal fluorescence laser scanning microscopy, pathway-specific markers, a range of endocytosis pathway-specific inhibition strategies, as well as MIF receptor overexpression and blockade approaches, we specifically wished to address the following questions: (i) is MIF endocytosed through the classical clathrin-dependent pathway or are other pathways involved; (ii) does MIF traffic to early and late endosomes upon uptake or is it recycled; (iii) does MIF endocytosis occur in a receptor-mediated manner and are CD74 and CXCR4 involved; (iv) if MIF/receptor complexes are efficiently internalized, does MIF signaling occur from the plasma membrane or can MIF signal from within endosomal compartments?

Materials and methods

Cells, antibodies, plasmids, and reagents

Mouse embryonic fibroblasts (MEFs), human embryonic kidney cells (HEK293), human dermal fibroblasts (F277; a kind gift from Dr. Jens Baron, Department of Dermatology, RWTH Aachen University), and the HeLa-derived cell line HtTA1 (Nguyen et al., 2003) were grown in Dulbecco's modified Eagle medium (D-MEM)

supplemented with GlutamaxTM, containing 4.5 g/l D-glucose and sodium pyruvate, 10% fetal calf serum (FCS), and 1% penicillin/streptomycin (P/S). The monocyte cell line THP-1, the human T cell line Jurkat, and the human T/NK cell leukemia cell line YT2C2 were grown in RPMI 1640 medium, containing 10% FCS and 1% P/S. YT2C2 cells were a kind gift from Dr. Kendall Smith (Cornell University's Weill Medical College). MonoMac6 cells were cultured in RPMI 1640 medium containing 10% FCS, 1% P/S, 1% non-essential amino acids (NEAA), 9 µg/ml human insulin (Sanofi-Aventis, Paris, France) and 1 mM sodium pyruvate. MDA-MB231 cells were cultured in D-MEM, containing 10% FCS, 1% P/S, 2 g/l D-glucose and 1% L-glutamine. Unless stated otherwise, all cell culture reagents including media and supplements were from Invitrogen (Karlsruhe, Germany).

For the analysis of clathrin or caveolin levels, mouse monoclonal antibody to clathrin light chain [CON.1] from Abcam (ab24579) and rabbit polyclonal caveolin-1 antibody (N-20) from Santa Cruz Biotechnology (sc-894) were used. For the signaling assays, anti-phospho-AKT antibodies (Ser473 and Thr308) from Cell Signaling (Danvers, MA, USA) were used. A mouse monoclonal anti-actin antibody (clone C4 from MP Biomedicals, Irvine, CA, USA) was used as loading control. The mouse anti-CXCR4 antibody MAB171 from R&D Systems (Heidelberg, Germany) was used to neutralize CXCR4. pEGFP-C1-Rab7, pUHG16wtdynamin and pUHG16K44A dynamin were a kind gift from Dr. Marino Zerial (Max-Planck-Institute Dresden). The CD74 expression plasmid pCD74minRTS, encoding for a human CD74 gene devoid of the ER retention signal, as well as the fluorescently tagged constructs pEYFP-C1-CD74, pECFP-N1-CXCR4 and pEYFP-C1-CD74minRTS have been described (Schwartz et al., 2009). The CD74 over-expression plasmid pcDNA3.1/V5-His-TOPO-CD74 has also been described (Leng et al., 2003). The selection plasmid pBABEpuro was obtained from Dr. B. Lüscher (RWTH Aachen University, Germany) and was originally from Addgene.

The following pharmacological inhibitors, fluorescent probes, and chemicals were used: AMD3100, doxycyclin, phorbol 12-myristate 13-acetate (PMA, P8139-M6), bafilomycin A1, nocodazole (Sigma, München, Germany); puromycin (Calbiochem/Merck, Darmstadt, Germany). The endocytosis inhibitors monodansylcadaverine (MDC), dynasore monohydrate, nystatin, and filipin III were all obtained from Sigma. Chlorpromazine (CPZ) was purchased from Calbiochem/Merck. Alexa488-acLDL, Alexa488-transferrin, and Alexa488-cholera toxin were from Invitrogen.

Cell transfection assays

For transient transfections of HEK293 or HtTA1 cells, FuGENE HD reagent from Roche Diagnostics (Basel, Switzerland) was used. MEFs were electroporated by using Amaxa nucleofector II (Cologne, Germany).

Labeling of recombinant human MIF (rMIF)

Biologically active recombinant human MIF (rMIF) was prepared as described and contained negligible concentrations of endotoxin (<10 pg endotoxin/µg MIF) (Bernhagen et al., 1994). Freshly renatured rMIF was then labeled with AlexaFluor 546 (Invitrogen). Unincorporated dye was removed by gel filtration.

Colocalization experiments by fluorescence microscopy, temperature shift, and live imaging studies

Microscopy was performed by high resolution fluorescence with an IX50 Olympus or by laser scanning fluorescence microscopy with an LSM710 laser scanning confocal microscope (LSM) or with an LSM510 (both from Zeiss). Routine analyses were performed with

the IX50. Quantification of colocalizing fluorescent proteins and/or endocytotic events was done by visual cell counting and using the CellF quantification software (Olympus).

HEK293 cells (1×10^6) or MEFs (2×10^6) were seeded, transfected with pEGFP-C1-Rab7 and cells grown for 24 h (HEK293) or 48 h (MEFs) at 37 °C. After detachment and centrifugation at 1250 rpm for 5 min, cells were resuspended in medium and seeded on cover slips. Twenty-four hours later, cells were pretreated with one of the endocytosis inhibitors (MDC, 50 µM; CPZ, 50 µM; or dynasore 80 µM for HEK293 or additionally nystatin, 50 µg/ml; filipin, 5 µg/ml; bafilomycin, 200 nM; or nocodazole, 20 µM for MEFs) or left untreated and incubated for 30 min (MDC, CPZ, bafilomycin, nocodazole) or 1 h (nystatin, filipin) before adding Alexa⁵⁴⁶MIF (200 ng/ml) or control buffer for different time periods at 37 °C. Then, cells were placed on ice, medium aspirated, and cells washed with ice-cold glycine buffer, pH 2.8, and ice-cold PBS, before fixation (3.6% paraformaldehyde) and mounting on microscope slides.

For temperature shift experiments, HEK293 cells (2×10^6) were cultured 1 day before transfection with pEGFP-C1-Rab7. Twenty-four hours post transfection, cells were detached, centrifuged, seeded onto cover slips and incubated at 37 °C overnight. The next day, cells were incubated at 4 °C for 10 min and Alexa⁵⁴⁶MIF (1 µg/ml) was added and cells were incubated for 1 h at 4 °C to allow equilibrium binding of MIF to cell surface receptors. Medium was replaced by cold medium. The temperature was then shifted from 4 °C to 37 °C and cells were allowed to internalize for 10–120 min, before washing, fixation, and mounting.

For live imaging, HEK293 cells (5×10^5) were grown on poly-L-lysine-coated cover slips. A cover slip was mounted in a heated chamber (37 °C, 5% CO₂) onto an LSM510 confocal microscope. Imaging started immediately after the addition of Alexa⁵⁴⁶MIF (1 µg/ml) and/or Alexa⁴⁸⁸cholera toxin b (10 µg/ml). MEFs (2×10^6) were transfected with pEGFP-C1-Rab7 and seeded 2 days before live imaging. Images were taken every 4 min.

For colocalization analyses, HEK293 cells (2×10^5) were seeded onto cover slips and incubated overnight at 37 °C. Upon equilibration to 4 °C (10 min), Alexa⁵⁴⁶MIF (1 µg/ml) together with Alexa⁴⁸⁸acLDL (5 µg/ml) or Alexa⁴⁸⁸transferrin (25 µg/ml) were simultaneously added. Cells were incubated for 30 min at 4 °C. Then, medium was replaced with cold medium and the temperature shifted from 4 °C to 37 °C and cells were allowed to internalize for 2–180 min (for acLDL) or 2–30 min (for transferrin). Colocalization between MIF and acLDL or transferrin was analyzed by confocal microscopy using the LSM710.

For analysis of the colocalization between MIF and its receptors CXCR4 and CD74, HEK293 cells (2×10^6) were seeded, transfected with pECFP-N1-CXCR4 and pEYFP-C1-CD74minRTS or pEYFP-C1-CD74, respectively, and grown for 24 h at 37 °C. The next day, cells were detached and seeded onto cover slips and incubated at 37 °C overnight. Twenty-four hours later, the cells were incubated with Alexa⁵⁴⁶MIF (1 µg/ml) for 30, 60 or 120 min, washed, fixed, and mounted as before, and inspected by confocal microscopy using the LSM710.

Inhibition of dynamin by expression of a dominant-negative construct

pUHG16-3 is a Tet-response plasmid used for inducible expression of amino-terminal HA-epitope-tagged dynamin or dominant-negative variants thereof. The binding of tetracycline (tet) or doxycycline (doxy) to the transactivator (VP16-TetR) which is constitutively expressed in transformed HtTA1 cells regulates the expression of dynamin (Damke et al., 1994; Nguyen et al., 2003). K44A is a point mutation in one of the GTP-binding elements of dynamin and inactivates dynamin in a dominant-negative manner. HtTA1 cells were seeded and allowed to grow in D-MEM,

containing doxy at 1 $\mu\text{g/ml}$. The next day, cells were transfected with pBABEpuro, pEGFP-C1-Rab7, and either pUHG16wtdynamin or pUHG16K44Adynamin and incubated for 24 h at 37 °C and 5% CO₂. Medium was changed and cells were selected with puromycin (5 $\mu\text{g/ml}$; 37 °C; overnight) and seeded on cover slips. Additionally, two wells were left untreated to activate the expression of either wildtype or K44A-dynamin from the transfected dynamin plasmid. To the two control plates, doxycyclin (1 $\mu\text{g/ml}$) was added to switch off the expression of the plasmid. Expression of ectopic proteins proceeded for 2 days before HtTA1 cells were treated with Alexa⁵⁴⁶MIF (200 ng/ml) for different time periods, and washed, fixed, and mounted as above.

Analysis of caveolin and clathrin levels by Western blotting

Cells (2×10^5) of each cell line (HEK293, YT2C2, MEF, THP-1, MDA-MB-231, HtTA1 and MonoMac6) were seeded and incubated for 24 h at 37 °C. Additionally, THP-1 cells were differentiated into macrophages by the addition of PMA (100 ng/ml; 24 h; 37 °C). Cells were lysed in LDS sample buffer, boiled and sonified. Samples were separated by SDS-PAGE, transferred to nitrocellulose membranes and clathrin or caveolin revealed with adequate antibodies. Western blotting was performed essentially as described (Bernhagen et al., 2007). Actin was used as a loading control. Ratios of caveolin-1 or clathrin to actin were calculated by band densitometry using Aida Image Analyzer Software (Raytest Isotopen, Berlin, Germany).

MIF uptake studies after receptor overexpression and blockade

To study the dependence of MIF internalization on CD74, HEK293 cells or HtTA1 cells were seeded 24 h before transfection with either pCDNA3.1/V5-His-TOPO-CD74, pBABEpuro and pEGFP-C1-Rab7 (ectopic CD74 overexpression) or with pBABEpuro and pEGFP-C1-Rab7 (control). The next day, cells were selected by addition of puromycin (5 $\mu\text{g/ml}$) for 24 h at 37 °C. Following seeding on cover slips, Alexa⁵⁴⁶MIF (200 ng/ml) was added for different time periods, and cells washed, fixed, and mounted as above.

Dependence of MIF internalization on CXCR4 was additionally checked with the specific inhibitor AMD3100. HEK293 cells were seeded 24 h before they were transfected with pCD74minRTS and pEGFP-C1-Rab7 or with pEGFP-C1-Rab7 alone (control). Twenty-four hours later, cells were detached, centrifuged, resuspended in full medium, and seeded on cover slips. After another 24 h at 37 °C and 5% CO₂, cells were either left untreated or were pretreated with AMD3100 (10 $\mu\text{g/ml}$) for 30 min at 37 °C before incubation with Alexa⁵⁴⁶MIF (1 $\mu\text{g/ml}$) for different time periods. Washing and fixing was done as before.

Signaling experiments

For EGF-stimulated AKT signaling experiments, HtTA1 cells (10^5 /well) were seeded in D-MEM medium containing 10% FCS and grown for 24 h at 37 °C. Before EGF addition, cells were incubated for 24 h under low serum condition (0.5% FCS). Scouting experiments indicated that 100 ng/ml recombinant human EGF (huEGF) was optimal for inducing AKT in these cells. Cells were pretreated with 5, 8, 10 or 50 μM of CPZ for 30 min at 37 °C or left untreated before their stimulation with huEGF (100 ng/ml) for 10 min at 37 °C. Control cells received an equal volume of buffer.

MIF signaling experiments were performed in Jurkat T cells, HtTA1 cells, or human dermal fibroblasts (F277). As described for EGF-stimulated AKT signaling, cells (10^5 /well) were seeded and starved. Then, they were pretreated with 50 μM MDC, 5, 8, 10, 25 or 50 μM CPZ, or 80 μM dynasore for 30 min at 37 °C or left untreated before stimulation with huMIF (50 ng/ml) for 10 min at 37 °C or treatment with control buffer.

After signaling had occurred, cells were centrifuged, lysed and prepared for SDS-PAGE/Western blot analysis using an anti-phospho-AKT antibody (Ser473 or Thr308). AKT activity was measured with the *in vitro* AKT kinase assay from Cell Signaling. Jurkat cells were treated with endocytosis inhibitors and rMIF as described above. Activated phosphorylated AKT was then selectively immunoprecipitated with a bead-immobilized rabbit anti-phospho-AKT antibody (D9E). The resulting immunoprecipitate was incubated with a GSK3 α/β fusion protein ('the substrate') in the presence of ATP and kinase buffer. Phosphorylation of the substrate was then measured by Western blotting analysis using an anti-phospho-GSK-3 α/β (Ser21/9) rabbit mAb (37F11). Phosphorylation ratios (phospho-AKT/actin or phospho-GSK) were calculated by band densitometry using Aida Image Analyzer Software.

Statistical analysis

Data are expressed as means \pm SD. Student's *t*-tests (two-sided, unpaired) were performed to compare experimental groups. Differences with a value of $p < 0.05$ were considered statistically significant.

Results

MIF is rapidly endocytosed and colocalizes with early and late endosomes

The precise mechanism of MIF internalization is poorly understood. In particular, the involved routing sub-pathways and receptors have remained ill-defined. We first wished to analyze MIF endocytosis in MEFs, which have been amply shown to elicit various MIF-driven signaling pathways, e.g. PI3K/AKT signaling (Lue et al., 2007). MEFs were incubated with rMIF which was fluorescently labeled with the dye AlexaFluor⁵⁴⁶. Alexa or FLUOS labeling of MIF has previously been shown to be compatible with the biological activity of MIF (Kleemann et al., 2002; Leng et al., 2003). Alexa⁵⁴⁶MIF at a concentration of 200 ng/ml was added and cells were further incubated for 30 and 60 min at 37 °C. Prominent fluorescent signals were observed within the MEFs at both time points, while negligible staining at 0 min and an applied rigorous acid washing procedure assured that the observed Alexa⁵⁴⁶MIF signal was intracellular and not due to non-specific interactions with the cell surface. This indicated that MIF had been efficiently internalized (Fig. 1A). These data convincingly confirmed earlier data which had demonstrated MIF endocytosis in macrophages, HeLa and NIH/3T3 cells (Berndt et al., 2008; Kleemann et al., 2000, 2002; Lue et al., 2006), and also showed that low physiological concentrations of exogenous MIF are rapidly internalized in primary fibroblasts and appear to localize to vesicle-like structures. Of note, MEFs express low-to-medium levels of the MIF receptors CXCR4 and CD74, respectively, as indicated by FACS and Western blot analysis (data not shown). We next asked whether MIF endocytosis would be detectable at earlier time points below 30 min. Internalization of Alexa⁵⁴⁶MIF was measured 5, 10, 20, and 30 min after addition and cell nuclei were co-stained for orientation. Vesicle-like Alexa⁵⁴⁶MIF-positive structures were already detectable after 10 min and were clearly appreciable after 30 min (Fig. 1B).

These data suggested that MIF had entered the endosomal pathway, with the vesicle-like structures supposedly representing early and/or late endosomal vesicles. To address this notion further, we performed temperature shift assays in which we transfected HEK293 cells with a Rab7GFP-plasmid (marker for late endosomes). Wildtype HEK293 cells are devoid of CD74, but express medium levels of CXCR4. Cells were pre-incubated at 4 °C and potential equilibrium binding of Alexa⁵⁴⁶MIF (1 $\mu\text{g/ml}$) to cell surface

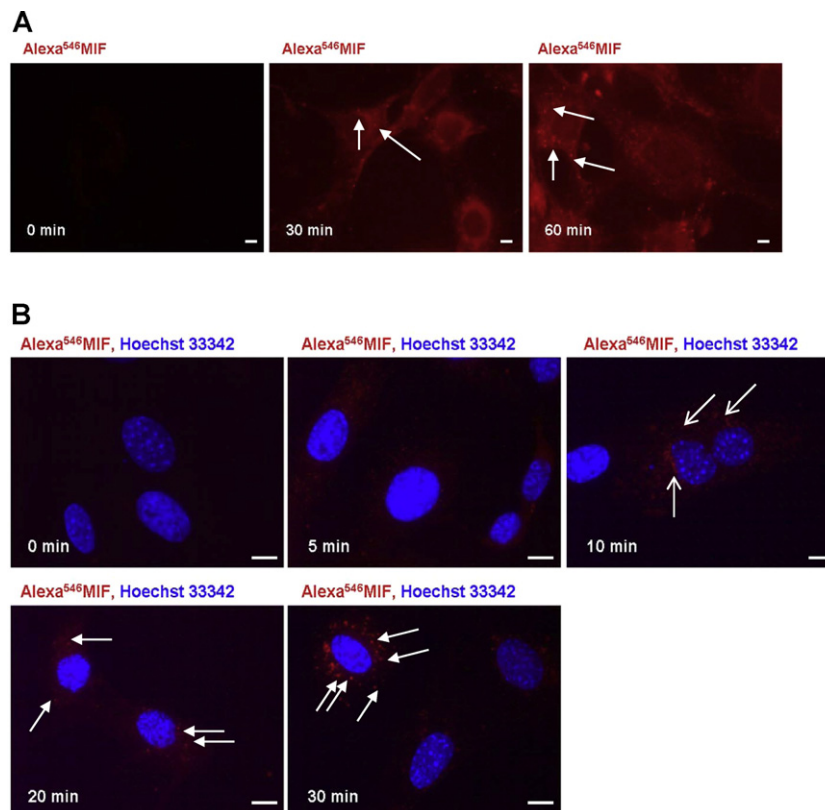


Fig. 1. MIF is rapidly endocytosed in mouse embryonic fibroblasts (MEFs) and localizes to vesicle-like structures. (A) MEFs were incubated with AlexaFluor⁵⁴⁶-labeled human MIF (200 ng/ml) for 0, 30 or 60 min, cells rigorously washed (acid wash at pH 2.8), fixed, and mounted for microscopic examination using a high resolution fluorescent microscope from Olympus. (B) Same as in (A) except that early time intervals were included and cells were co-stained with a nuclear marker (blue). Endocytosed MIF (red) and MIF-positive vesicle-like structures are indicated by arrows. Scale bars: 10 μ m. Fixation of the cells was performed at the time points indicated.

receptors was allowed to occur for 1 h at 4 °C. Upon temperature shift to 37 °C, uptake of MIF was followed from 0 to 120 min. Fig. 2A shows representative microscopic images, indicating colocalization between MIF and Rab7 by orange/yellowish overlay fluorescence signals. Depending on the focus layer, MIF/Rab7 colocalization was either apparent by yellowish overlay color or by reddish Alexa⁵⁴⁶MIF staining within green Rab7-positive vesicle-/ring-like compartments. Colocalization between MIF and the late endosomal compartment was confirmed by quantitative analysis. Analysis was both performed by visual inspection and counting of those cells which showed colocalization between the marker protein and MIF (Fig. 2B; as defined in detail in the section “Materials and methods”) and by applying the Cell^F software for quantification of fluorescence-positive cell areas (Fig. 2C). Analysis by either method revealed that endocytosed MIF markedly and significantly colocalized with Rab7-positive late endosomal vesicles (Fig. 2B and C). Colocalization was evident as early as 10 min after temperature shift, was most prominent after 30 min, and plateaued thereafter. A similar type of colocalization was observed between MIF and Rab5 (a marker for early endosomes) upon transfection of the Rab5GFP-plasmid. Although colocalization between MIF and the early endosome marker may have been expected to occur even earlier than that for Rab7, convincing colocalization was not seen until 10 min after temperature shift and thereafter appeared to plateau (data not shown), an observation possibly in line with the two populations of early endosomes (static and dynamic) as suggested by Lakadamyali et al. (2006).

To simulate the physiological situation of a cytokine binding to its membrane receptor(s) of a given target cell, additional endocytosis experiments were performed in cells that were exposed to exogenous Alexa⁵⁴⁶MIF and continuously observed for 10–120 min

under physiological temperature conditions. As seen above under temperature shift conditions (Fig. 2A), addition of 200 ng/ml Alexa⁵⁴⁶MIF to transient HEK293-Rab7GFP transfectants under ambient conditions led to an observable colocalization between MIF and Rab7 between 10 and 120 min (data not shown). For confirmation and closer analysis, live imaging on a laser scanning microscope was performed using living MEFs, which also had been transiently transfected with Rab7GFP. Images were taken every 4 min right after the addition of Alexa⁵⁴⁶MIF (Supplementary Fig. 1 and Suppl. Video 1). This analysis showed that colocalization between MIF and Rab7-positive late endosomes, as indicated by the appearance of greenish vesicles surrounding reddish MIF-derived fluorescence, was clearly detectable after 16 min. Also trafficking and maturation of these structures over a time course of 160 min was observable together with the formation of additional MIF-/Rab7-positive vesicles in a given cell.

In aggregate, these data suggested that MIF at physiological concentrations is rapidly internalized and targeted to late endosomes.

Endocytosis of MIF is clathrin- and dynamin-dependent and its transport through the endolysosomal compartment is microtubule-mediated and depends on functional acidification of endosomes

Based on the above findings, we next wished to define the precise mechanism and sub-pathway by which MIF is endocytosed. We thus applied numerous pathway-specific inhibitors and blockade strategies for the clathrin-associated and clathrin-independent pathways. We first performed Western blot analysis to check for clathrin protein expression levels in the cell types used and compared them with those of monocytes/macrophages, the cancer cell

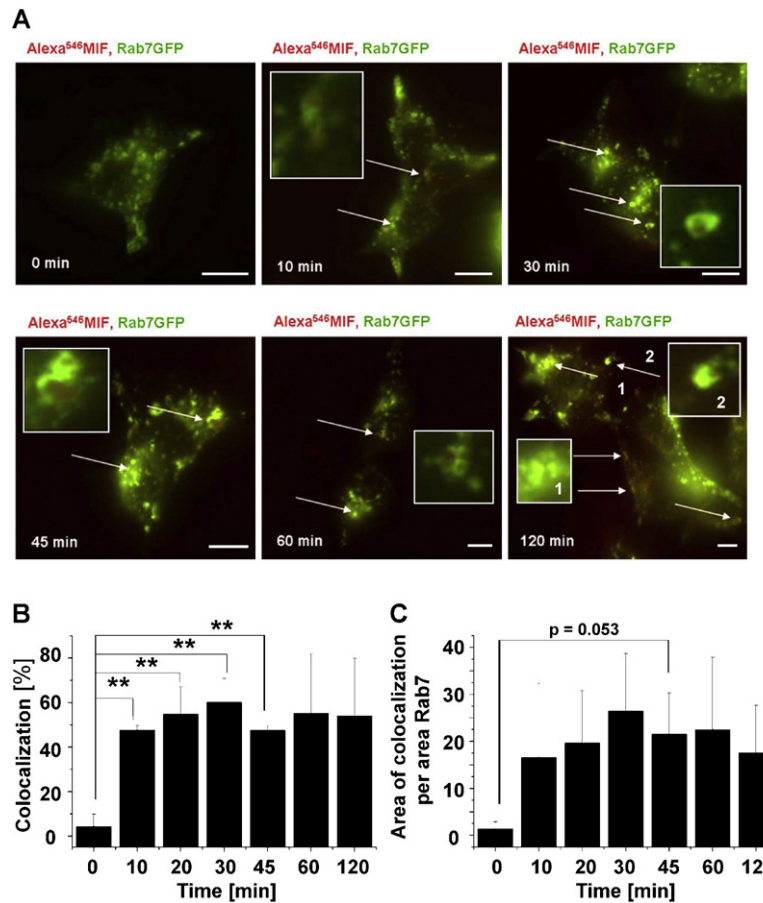


Fig. 2. MIF colocalizes with late endosomes in HEK293 cells. (A) Transient Rab7GFP HEK293-transfectants were incubated with AlexaFluor⁵⁴⁶-labeled human MIF (200 ng/ml) for the indicated time intervals, washed with glycine buffer pH 2.8, fixed, and mounted. Images show representative cells from a total of $n = 10$ independent experiments analyzed by conventional high resolution fluorescence microscopy. Arrows indicate colocalization between Rab7GFP and Alexa⁵⁴⁶MIF. Scale bars: 10 μ m. Insets represent magnifications. Colocalization is represented by green rings with red fillings and/or yellow overlay color. (B) As in (A) but applying temperature shift conditions, which allowed for synchronization of uptake processes and equilibrium MIF binding to cell surface receptors. Rab7GFP-HEK293 transfectants were incubated with Alexa⁵⁴⁶MIF (1 μ g/ml) for 1 h at 4 °C, washed with cold buffer, and the temperature shifted to 37 °C for the time intervals indicated. (B) Quantification of Alexa⁵⁴⁶MIF/Rab7GFP colocalization by counting positive cells per eye (100 cells per condition). (C) Quantification of Alexa⁵⁴⁶MIF/Rab7GFP colocalization by Cell^F software (Olympus). Results were obtained from three independent experiments. Asterisks indicate statistical significance (** $p < 0.01$).

line MDA-MB231 and YT2C2. The latter cell type is known to lack caveolin-1 expression. Fig. 3A indicates that all analyzed cell types express appreciable levels of clathrin. MEFs, HEK293 and HtTA1 cells were chosen for the subsequent pathway analysis.

Whether MIF endocytosis is clathrin-dependent was first tested by applying the pharmacologic inhibitor MDC, which specifically inhibits the membrane-bound enzyme transglutaminase type I and thus interferes with protein-protein crosslinking reactions and hence clathrin-mediated vesicle formation. MEFs, transiently transfected with pRab7GFP, were pre-treated with MDC before addition of Alexa⁵⁴⁶MIF, and colocalization between Alexa⁵⁴⁶MIF and Rab7 evaluated after 180 min. MDC markedly inhibited MIF endocytosis as indicated by lack of or reduced colocalization with Rab7-positive compartments. Fig. 3B shows a typical untreated cell, i.e. in which MIF localizes to a Rab7-positive endosome (as indicated by a green fluorescent ring with red fluorescent filling) and a typical MDC-treated cell, in which no or less colocalization was observed. Quantification of this experiment by counting out several hundred cells revealed that the achieved inhibitory effect of MDC was at around 30% (Fig. 3C). By comparison, the endocytosis of LDL, which follows the canonical clathrin-mediated pathway, could be inhibited by approximately 50–70% by MDC pre-treatment (data not shown). Nevertheless, the MDC inhibition experiments indicated that MIF is endocytosed in a clathrin-dependent manner. In fact, similar inhibition of MIF endocytosis was observed upon

pre-treatment of cells with CPZ, which directly interferes with clathrin coat formation (data not shown). To further confirm trafficking of MIF through a clathrin-dependent endocytosis pathway, the experiment was performed in Rab7GFP-transfected HEK293 cells as well. Fig. 3D shows that MIF endocytosis in these cells was significantly and markedly blocked by MDC essentially throughout the entire time interval of 120 min. Inhibition was maximal at 60 and 120 min after MIF addition, when it reached an inhibition rate of about 50%.

Clathrin-coated vesicles are known to be bud-off from the plasma membrane in a process mediated by the GTPase dynamin. Therefore, we next aimed at testing MIF endocytosis in the presence or absence of functional dynamin. Using Tet-regulated HeLa cells (HtTA1) for the MIF endocytosis experiments, the colocalization between Alexa⁵⁴⁶MIF and Rab7 was compared in control-transfected cells, cells transfected with dominant-negative (dn) dynamin, and those ectopically overexpressing wildtype dynamin. One-hundred and twenty minutes after Alexa⁵⁴⁶MIF addition, MIF/Rab7 colocalization was markedly increased in dynamin-overexpressing cells compared to control cells expressing endogenous dynamin levels only (Fig. 4A). In contrast, dynamin inactivation by expression of dn dynamin led to a decrease in MIF/Rab7 colocalization. The quantification indicated that the reduction of MIF/Rab7 colocalization by dn dynamin was significant after 120 min, whereas the observed increase in colocalization

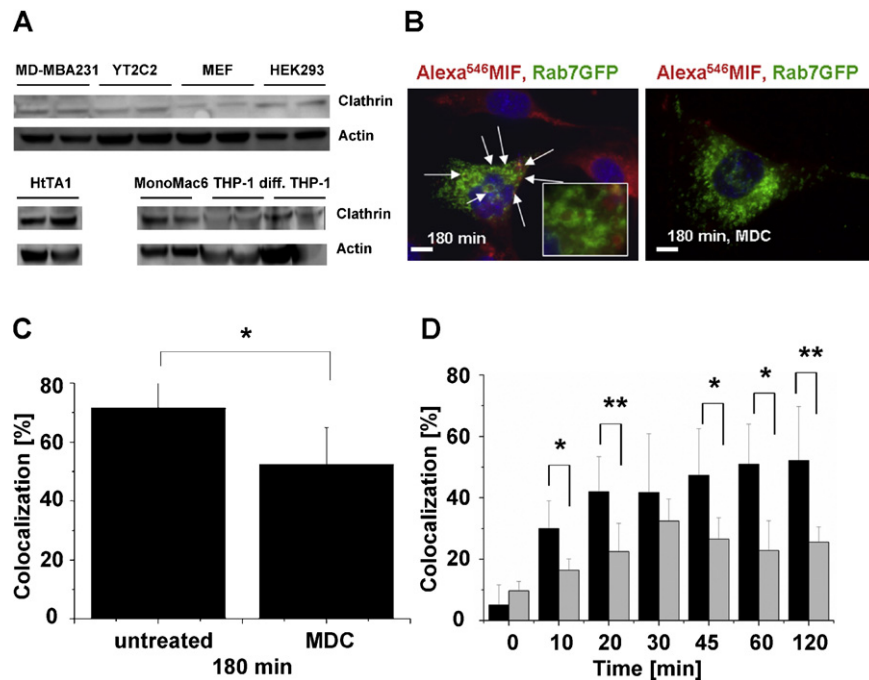


Fig. 3. MIF endocytosis is clathrin-dependent. (A) Analysis of clathrin protein levels in different cell lines by Western blotting using a mouse monoclonal antibody to clathrin light chain. Actin was used as a loading control. (B) Monodansylcadaverine (MDC) reduces MIF endocytosis in mouse embryonic fibroblasts (MEFs). MEFs transiently transfected with Rab7GFP were treated with MDC (50 μ M) or were left untreated for 30 min at 37 °C before adding AlexaFluor⁵⁴⁶-labeled human MIF (200 ng/ml) for 3 h at 37 °C. Following rigorous washing cells were analyzed by conventional fluorescence microscopy. Images show representative cells (left, untreated; right, treated with MDC). Arrows indicate colocalization between Rab7GFP and Alexa⁵⁴⁶MIF (represented by green rings with red fillings). Scale bars: 10 μ m. (C) Quantification of all images as analyzed in (B). Results represent means \pm SD of $n = 6$ independent experiments each (* $p < 0.05$). (D) MDC blocks MIF endocytosis in HEK293 cells. As in (C), except that images taken from experiments performed in MDC-treated HEK293 transfectants were quantitated. Incubation with Alexa⁵⁴⁶MIF was 0–2 h at 37 °C. Results represent means \pm SD of $n = 10$ (for untreated cells; black bars) and $n = 3$ (for MDC-treated cells; gray bars) independent experiments (* $p < 0.05$; ** $p < 0.01$).

was most apparent after 30 min, although it was not formally significant (Fig. 4B; $p < 0.01$ and $p = 0.05$, respectively). To further verify the involvement of dynamin in the endocytosis pathway of MIF, we next inhibited dynamin function in HEK293 cells by applying the cell-permeable inhibitor dynasore. This inhibitor strongly interfered with MIF endocytosis as indicated by significantly and markedly reduced MIF/Rab7 colocalization in dynasore- versus control solvent-treated cells 20, 45, 60 and 120 min after MIF addition. Dynasore-mediated inhibition of MIF uptake ranged from 36 to 62% (Fig. 4C and D). Thus, the studies with dn dynamin and dynasore together suggested that MIF endocytosis is dependent on functional dynamin, which also further confirmed trafficking of MIF along a clathrin-dependent endocytosis track, as dynamin is prominently involved in the clathrin-mediated endocytosis pathway.

The canonical clathrin-mediated endocytosis pathway involves microtubule-dependent endosomal vesicle transport and early-to-late endosomal maturation, which is coupled to an acidification process. We applied bafilomycin, which inhibits the vesicular proton pump and nocodazole, which blocks microtubule assembly/disassembly and tested the effect of these inhibitors on MIF endocytosis in MEFs following Rab7GFP transfection and Alexa⁵⁴⁶MIF. Both inhibitors led to an apparent arrest of MIF trafficking through the endocytic pathway followed by a swelling of the MIF-containing endosomal vesicles (Fig. 5). These experiments further underscored the notion that MIF endocytosis occurs through a canonical clathrin-dependent endocytic pathway.

Proteins internalized by a clathrin-dependent mechanism can follow different sub-pathways. For example, transferrin is recycled back to the plasma membrane from an endosomal compartment, whereas low density lipoprotein (LDL) is transported further to the lysosome, where it is degraded. On the other hand, toxins like the bacterial toxin cholera toxin B is internalized by a dynamin-dependent yet clathrin-independent pathway. We

directly compared the endocytosis process of MIF with that of transferrin, acetylated LDL (acLDL), and cholera toxin B by colocalization experiments in HEK293 cells which were exposed to the respective fluorescently labeled proteins. First, Alexa⁵⁴⁶MIF and Alexa⁴⁸⁸acLDL were simultaneously added to the cells and colocalization followed over a time course of 180 min, including early time intervals at 2, 5, 10, and 15 min. Marked colocalization between MIF and LDL was first observed after 30 min, and became even more prominent after 60, 120, and 180 min (Fig. 6A). Only weak colocalization with LDL could be seen within the first 30 min. In contrast, there was an early colocalization between Alexa⁵⁴⁶MIF and Alexa⁴⁸⁸transferrin within 5–10 min after endocytosis which however vanished after 30 min (Fig. 6B). Alexa⁵⁴⁶MIF and Alexa⁴⁸⁸cholera toxin B did not colocalize at any time during the endocytotic process (Fig. 6C). We conclude that internalized MIF enters an early endosomal pathway which it shares with proteins such as transferrin, but then enters the late endosomal/lysosomal pathway comparable with LDL rather than being recycled back to the plasma membrane. Complete lack of colocalization between MIF and cholera toxin B further confirmed the notion that MIF endocytosis is clathrin-dependent and does not follow other pathways such as the caveolin-dependent track.

This latter assumption was further probed by studying the effect of nystatin and filipin, both inhibitors of clathrin-independent pathways via caveolae and lipid rafts. We first tested and verified caveolin-1 protein levels in various cell types by anti-caveolin-1-specific Western blotting analysis. MEFs showed high caveolin-1 expression and were deemed suitable for our purpose (Supplementary Fig. 2A). Neither nystatin nor filipin influenced MIF endocytosis significantly compared to untreated cells (Supplementary Fig. 2B), corroborating that MIF endocytosis does not follow a caveolin-dependent pathway.

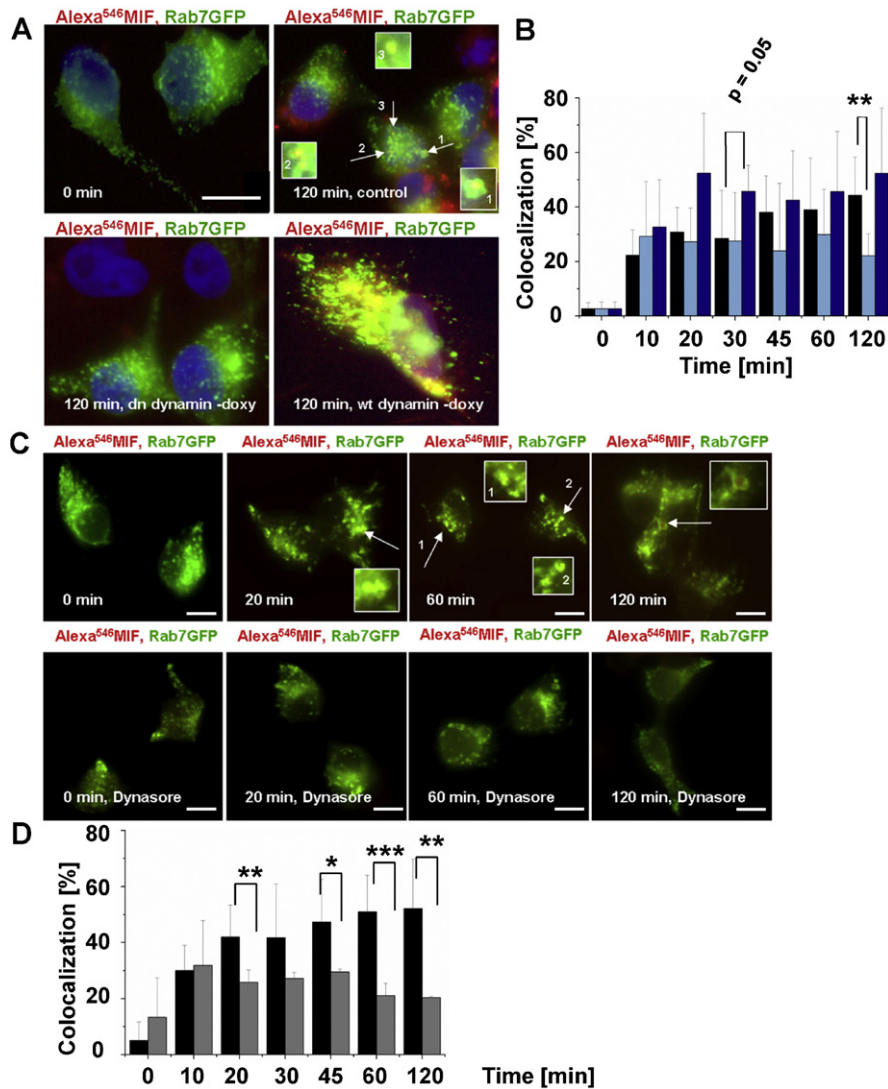


Fig. 4. MIF endocytosis depends on functional dynamin. (A and B) Expression of dominant-negative (dn) dynamin inhibits MIF endocytosis in HeLa-type cells. (A) HtTA1 cells were transfected with pBABEpuro, pRab7GFP and either pUHG16wtDynamin (wildtype (wt) dynamin-doxo; bottom right) or pUHG16K44Adynamin (dn-dynamin-doxo; bottom left) and selected with puromycin. Expression of wt or dn dynamin was activated by removal of doxycyclin (doxy) or expression switched off by maintaining doxy levels (control). Uptake of Alexa⁵⁴⁶MIF (200 ng/ml) was followed for 2 h. Representative images are shown. Colocalization between Rab7GFP and Alexa⁵⁴⁶MIF is represented by green rings with red fillings and/or yellow overlay color. Insets are magnifications as indicated. Scale bar: 10 μ m. (B) Quantification of the experiments in (A). Black bars, control cells; light blue bars, cells expressing dn dynamin; dark blue bars, cells expressing additional wt dynamin. Results represent means \pm SD from $n = 4$ independent experiments for each condition (** $p < 0.01$). (C and D) The dynamin inhibitor dynasore inhibits MIF endocytosis in HEK293 cells. Similar as in (A and B), except that HEK293 cells were treated with dynasore or control buffer instead of dynamin constructs. Endocytosis of Alexa⁵⁴⁶MIF (200 ng/ml) was followed for 2 h. (C) Representative images of dynasore- (lower panel) and buffer-treated (upper panel) cells. Colocalization between Rab7GFP and Alexa⁵⁴⁶MIF is represented by green rings with red fillings and/or yellow overlay color. Scale bars: 10 μ m. (D) Quantification of (C). Results represent means \pm SD from $n = 3$ (dynasore-treated; gray bars) and $n = 10$ (control-treated; black bars) independent experiments (** $p < 0.01$; *** $p < 0.001$).

Role for CD74 and CXCR4 in MIF endocytosis

We next wished to clarify the role of the MIF receptors CD74 and CXCR4 in MIF internalization. CD74 is known to undergo rapid cycles of internalization and recycling. This results in a high cell surface turnover and only low numbers of CD74 molecules present at the surface at a given time point. CD74 should thus be ideally suited to support and promote MIF endocytosis.

We ectopically overexpressed CD74 in HEK293 cells and compared the internalization of Alexa⁵⁴⁶MIF in these cells with the uptake in control cells which do not express CD74. Overexpression of CD74 led to an increase of Alexa⁵⁴⁶MIF colocalization with Rab7GFP by about 32% at 10 min, while this difference leveled off at later time points. This indicated that MIF endocytosis is accelerated within the first minutes when CD74 is present (Fig. 7A and B). To probe these results further, the experiment was repeated in HtTA1

cells. These cells which are CD74-negative in their non-transfected state, showed a dramatic increase of Alexa⁵⁴⁶MIF/Rab7GFP colocalization (>3-fold) after 10 min upon ectopic CD74 expression, while again no significant increase in colocalization was seen at the later time points, confirming that CD74 leads to a marked acceleration of early MIF endocytosis processes (Fig. 7C and D).

The cells used in this study are known to endogenously express the MIF receptor CXCR4. Also, it has been demonstrated that CD74 and CXCR4 can form a heteromeric receptor complex in monocytes, T cells, and cell lines, when coexpressed in a given cell. Thus, we were interested in the potential colocalization between CD74 and CXCR4 in the MIF endocytosis pathway and a potential functional interplay. HEK293 cells were transiently co-transfected with YFP-CD74 (or YFP-CD74minRTS; this latter construct had been found to exhibit improved surface expression of CD74; see Schwartz et al., 2009) and CXCR4-CFP. Colocalization between

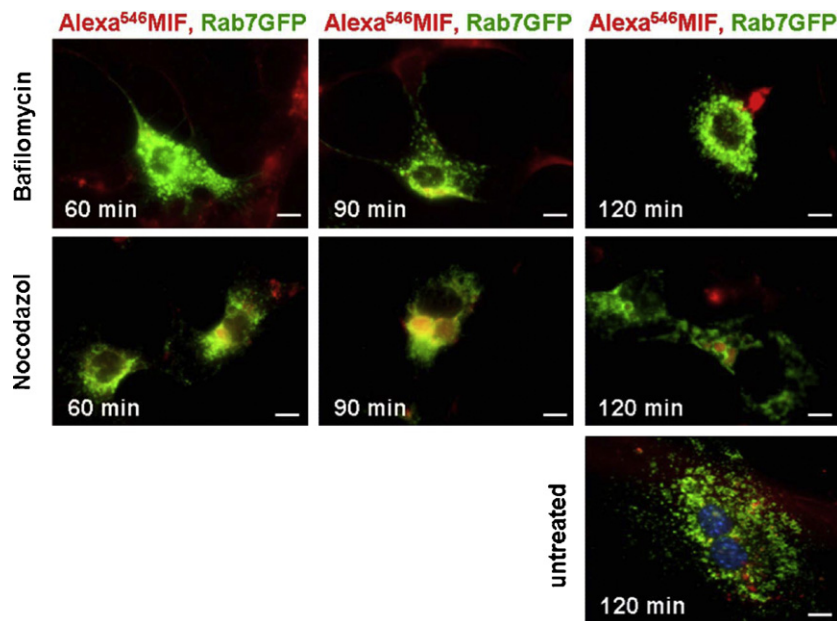


Fig. 5. Endocytotic trafficking of MIF is microtubule-dependent and requires endosomal acidification. Endocytosis of Alexa⁵⁴⁶MIF was followed in mouse embryonic fibroblasts (MEFs) transiently transfected with Rab7GFP for 2 h in the presence versus absence of the vesicular proton pump inhibitor bafilomycin or the microtubule assembly inhibitor nocodazole. Representative images from two independent experiments showing the inhibitory and arrest or swelling effect of these inhibitors are displayed. Colocalization between Rab7GFP and Alexa⁵⁴⁶MIF is represented by yellow overlay color. Blue staining in control cells (untreated) is due to nuclear staining with Hoechst33342.

both receptors and MIF was then followed upon addition of Alexa⁵⁴⁶MIF for 120 min using confocal laser scanning microscopy. Colocalization between YFP-CD74, CXCR4-CFP, and Alexa⁵⁴⁶MIF was observed 30 min after addition of Alexa⁵⁴⁶MIF but was mostly intracellular (data not shown). To make sure that CD74 was predominantly localized at the plasma membrane at the time point of Alexa⁵⁴⁶MIF addition, the experiment was redone transfecting YFP-CD74minRTS instead of YFP-CD74. Strong colocalization between CXCR4-CFP, YFP-CD74minRTS, and Alexa⁵⁴⁶MIF was seen 120 min after the addition of Alexa⁵⁴⁶MIF as indicated by white overlay staining (Fig. 8A). Colocalization was observed both at the plasma membrane as well as in vesicle-like intracellular compartments, indicating that both receptors participate in the endocytosis process of MIF.

To further test an involvement of CXCR4 in MIF endocytosis, the functional role of endogenous CXCR4 was examined in CD74-dependent MIF endocytosis in HEK293-CD74 transfectants by adding the CXCR4-specific bicyclam inhibitor AMD3100. Blockade of CXCR4 by AMD3100 led to a small yet significant reduction of about 20% in the HEK293-CD74 transfectants, whereas in untransfected cells which only express CXCR4, a larger blockade of 40% was observed. The latter result is of note, because it indicates that CXCR4 is involved in the endocytotic process of MIF. The partial reversal of this effect by ectopic CD74 expression suggests that CXCR4 and CD74 influence each other in their contribution to MIF endocytosis by forming a complex (Fig. 8B).

MIF-stimulated AKT signaling is at least partially dependent on endocytosis

It has become apparent that cytokine signaling may not only be initiated from a plasma membrane receptor activated by a cytokine, but also upon endocytosis of the ligated receptor. The latter process has been known as endosomal signaling. As both CXCR4 and CD74 contribute to MIF endocytosis and as CD74/CXCR4 complexes have previously been found to activate the PI3K/AKT pathway (Schwartz et al., 2009), we tested whether MIF-triggered PI3K/AKT signaling occurs from the plasma membrane or upon endocytosis.

Endosomal AKT signaling is well documented for epidermal growth factor (EGF). We verified the endosomal signaling effect of EGF in our HtTA-1 cells, as these cells express the EGF receptor in appreciable amounts. EGF dose-dependently increased AKT phosphorylation at residue Ser473 with a maximum stimulation occurring at a concentration of 100 ng/ml (phosphorylation ratio = 2.9). Of note, co-incubation with CPZ dose-dependently inhibited EGF-triggered AKT signaling and 50 μ M CPZ led to a significant and complete blockade of the response, showing that AKT activation by EGF was due to an endosomal signaling mechanism (Supplementary Fig. 3A). Recombinant MIF also induced AKT phosphorylation in HtTA-1, but the margin of this response was sub-optimal (phosphorylation ratio = 1.5) and variable. Also, CPZ had a dose-dependent effect on the baseline phosphorylation of AKT in the absence of exogenously added MIF. Endogenous MIF is known to activate the AKT pathway by an autocrine mechanism (Lue et al., 2007), thus indicating that CPZ may have interfered with autocrine MIF effects on the AKT pathway. Notwithstanding, CPZ markedly inhibited AKT activation by exogenously added MIF in a dose-dependent manner (Supplementary Fig. 3B). MIF-induced AKT phosphorylation was also inhibited by dynasore, AMD3100, and neutralizing anti-CXCR4 antibodies (Supplementary Fig. 3B), indicating together that AKT activation through the MIF/CXCR4 axis could at least in part be due to endosomal signaling processes. However, because the difference of the CPZ effect when one compared AKT activation by endogenous versus exogenous MIF was not prominent, we sought to confirm this initial finding in other cell types. Jurkat T cells have recently been shown to elicit a robust MIF-driven AKT response (Schwartz et al., 2009). We thus re-did the experiment in Jurkat cells. MIF-induced AKT phosphorylation (Ser473; phosphorylation ratio = 2.4) was blocked by MDC, CPZ and dynasore (Fig. 9A). Of note, the effect of CPZ was significant ($p < 0.05$) and the inhibitory effect of dynasore marginally lacked statistical significance ($p = 0.06$). AKT activation is frequently assessed by measuring the phosphorylation of Ser473, a C-terminal residue phosphorylated by mTOR and against which efficient antibodies are available. However, the phosphorylation of Thr308 is the actual activation loop phosphorylation which occurs during

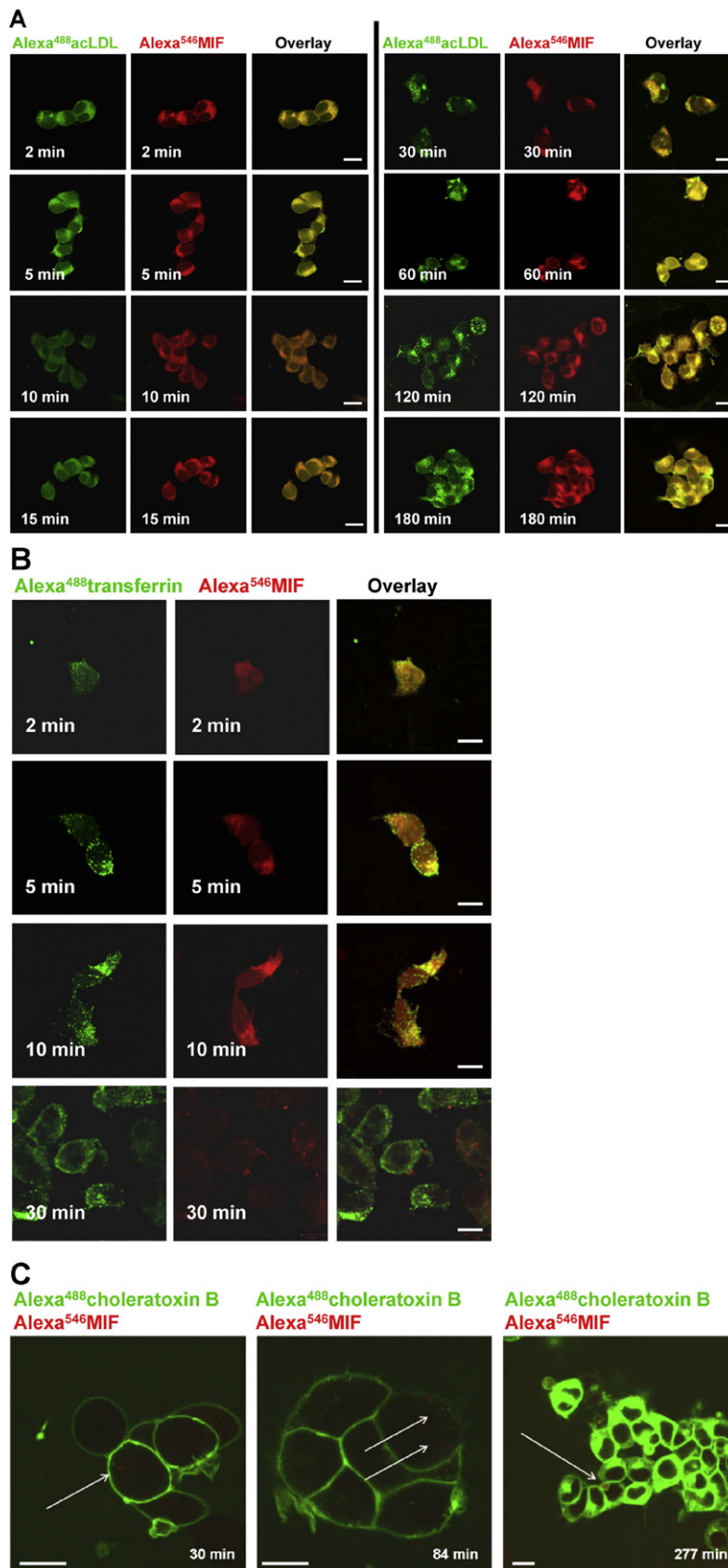


Fig. 6. During endocytotic passage MIF colocalizes with acLDL, partially with transferrin, but not with cholera toxin B. (A) The endocytotic pathway of MIF in HEK293 fully resembles that of acetylated low density lipoprotein (acLDL). Colocalization between Alexa⁵⁴⁶MIF (1 µg/ml) and Alexa⁴⁸⁸acLDL (5 µg/ml) was followed during the endocytotic process in HEK293 cells over a time course of 0–180 min. Incubation of cells with MIF and LDL occurred at 4 °C followed by a temperature shift to 37 °C. Colocalization was apparent by strong yellow overlay essentially over the entire time course. (B) Endocytosis of MIF in HEK293 cells colocalizes with that of transferrin at early time points (2–10 min), but pathways diverge thereafter. Alexa⁵⁴⁶MIF (1 µg/ml) and Alexa⁴⁸⁸transferrin (25 µg/ml) were simultaneously added to

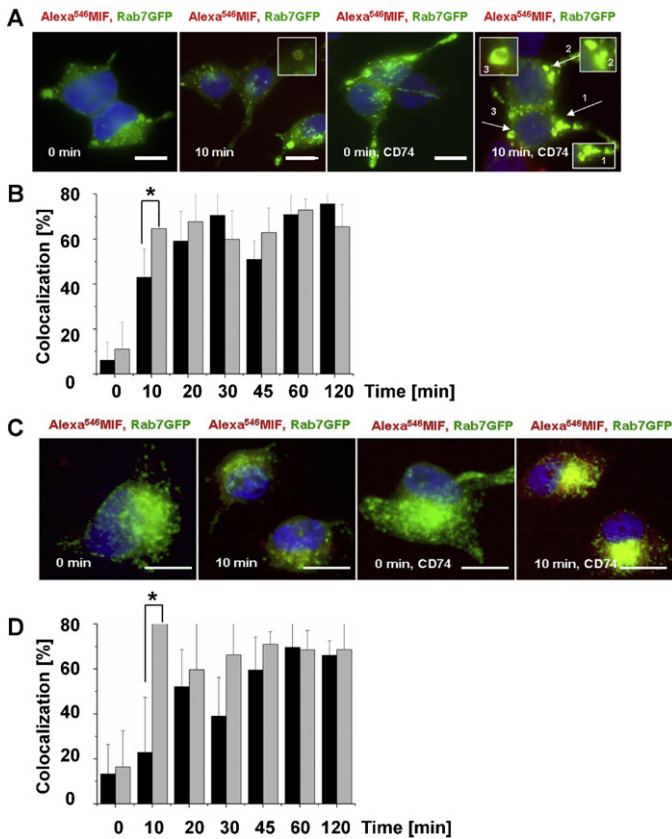


Fig. 7. Endocytosis of MIF is accelerated by ectopic CD74 overexpression. (A and B) HEK293 cells were transfected with either pcDNA3.1/V5-His-TOPO-CD74, pBABEpuro and pEGFP-C1-Rab7 (CD74) or with pBABEpuro and pEGFP-C1-Rab7 (control). Transfectants were selected with puromycin, Alexa⁵⁴⁶MIF (200 ng/ml) added, and endocytosis of MIF followed by detecting the colocalization with Rab7GFP by conventional high resolution fluorescent microscopic analysis. (A) Images showing representative cells from 4 independent experiments. Control cells (left) were compared to cells ectopically overexpressing CD74 (right). Arrows indicate colocalization between Alexa⁵⁴⁶MIF and Rab7GFP; numbered insets indicate magnifications. Cellular nuclei were co-stained with Hoechst33342. Scale bars: 10 μ m. (B) Quantification of (A). Black bars represent control cells, gray bars HEK293-CD74 transfectants. Results are means \pm SD of 4 independent experiments, with 100 cells counted for each condition (**p* < 0.05). (C and D) Same as (A and B) except that HeTA1 cells were examined. (A) Images show representative cells of 3 independent experiments. Control cells (left), HeTA1-CD74 transfectants (right). Yellow overlay staining indicates colocalization between Alexa⁵⁴⁶MIF and Rab7GFP. Nuclei of cells were stained with Hoechst33342. (D) Quantification of (C). Black bars represent control cells, gray bars HEK293-CD74 transfectants. Results are means \pm SD of 3 independent experiments, with 100 cells counted for each condition (**p* < 0.05).

AKT activation through PDK1. Thus, the blots were re-developed against Thr308 and the results essentially mirrored those obtained measuring the phosphorylation of Ser473 (Supplementary Fig. 4). Importantly, AKT activity was next directly probed by an *in vitro* kinase assay using GSK3 α/β as a substrate following isolation of active AKT from the various MIF and endocytosis inhibitor-treated incubations. This analysis nicely confirmed the AKT phosphorylation analyses and showed that MIF-stimulated AKT kinase activity is markedly blocked by MDC, CPZ and dynasore (Fig. 9B). Thus, MIF-stimulated AKT activation occurs at least in part through an endosomal signaling track. However, it should also be noted that this effect is probably not universal, because no dependence

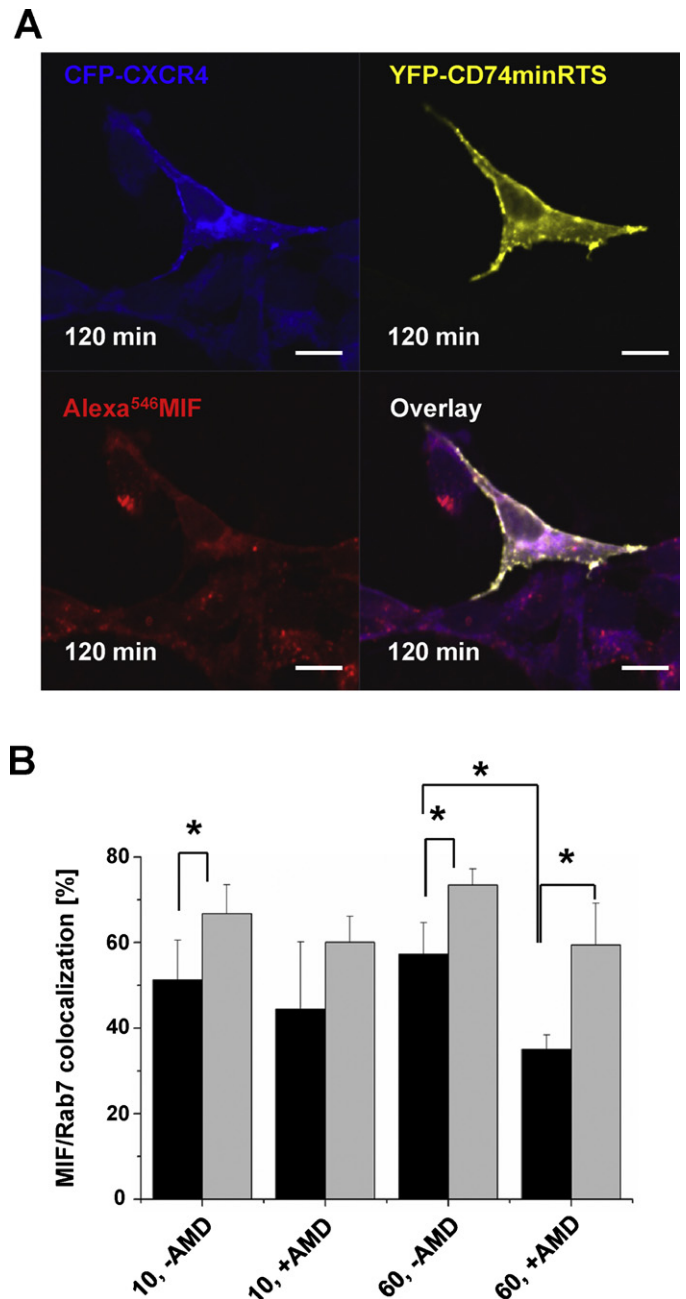


Fig. 8. CXCR4 participates in MIF endocytosis and colocalization of MIF, CD74, and CXCR4. (A) CD74, MIF, and CXCR4 colocalization in HEK293 cells both at the plasma membrane and in intracellular (endosomal) structures. HEK293 cells transfected with YFP-CD74minRTS and CXCR4-CFP were treated with Alexa⁵⁴⁶MIF (1 μ g/ml) and colocalization followed over 120 min. Representative images from 2 independent confocal microscopic analyses are shown. White-pinkish overlay color indicates colocalization between all 3 fluorophores. (B) Blockade of endosomal targeting of MIF by the pharmacological CXCR4-specific inhibitor AMD3100 (AMD; 10 μ g/ml) and partial rescue by ectopic CD74 expression. Endosomal localization of MIF was evaluated by counting cells showing a Rab7GFP/Alexa⁵⁴⁶MIF colocalization. Ten and 60 min time points after the addition of the fluorescently labeled MIF were taken. Quantification of all images was done by counting positive cells per eye. Black bars show control cells, gray bars HEK293 cells ectopically overexpressing CD74. Results represent means \pm SD of 4 independent experiments.

Fig. 6. cells at 4 $^{\circ}$ C, incubated and temperature was shifted to 37 $^{\circ}$ C to initiate endocytosis. Note that there is no colocalization seen any more after 30 min. (C) Endocytotic trafficking of MIF does not colocalize with that of the cholera toxin B pathway at any time. Colocalization between Alexa⁵⁴⁶MIF (1 μ g/ml) and Alexa⁴⁸⁸cholera toxin B (10 μ g/ml) was recorded over a 277 min endocytotic course in HEK293 cells. Living cells seeded on poly-L-lysine were used for this live imaging analysis. Microscopic analyses were performed using an LSM710 confocal fluorescence microscope. Images are representative of at least 3 independent experiments. Scale bars: 10 μ m. Arrows in (C) indicate areas of endosomal MIF staining which clearly does not colocalize with cholera toxin B.

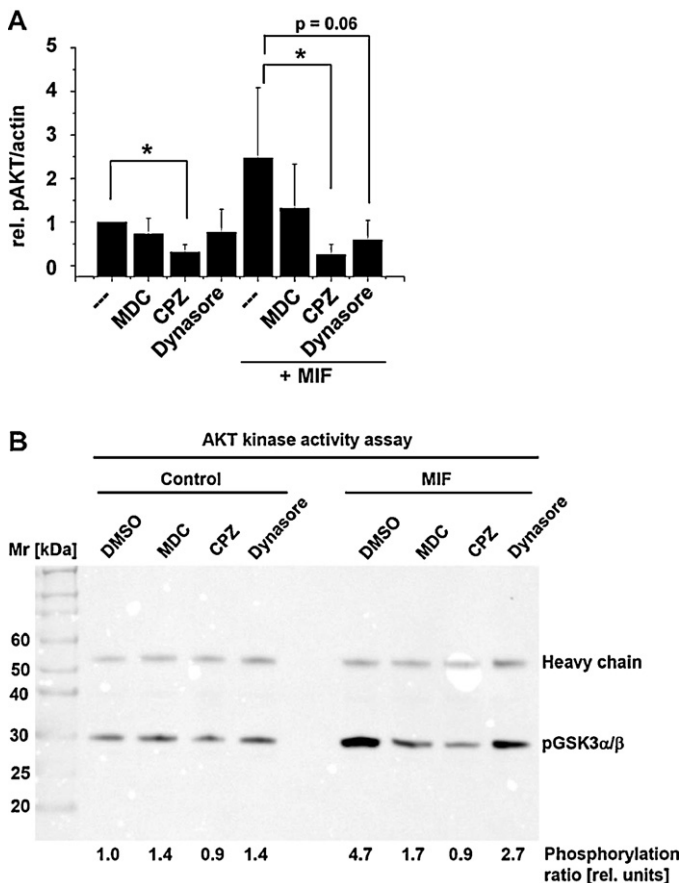


Fig. 9. MIF-stimulated AKT activation is partially due to endosomal signaling. (A) MIF-mediated AKT phosphorylation in Jurkat T cells is attenuated by inhibitors of clathrin-mediated endocytosis. Jurkat T cells were seeded and synchronized with medium containing 0.5% FCS. Cells were pretreated with MDC, CPZ, or Dynasore for 30 min or left untreated before incubation with human MIF (50 ng/ml; + MIF) or control buffer for 10 min as indicated. Phosphorylation ratios (pAKT over actin) were determined by anti-phospho-AKT (Ser473) and anti-actin Western blot and band densitometry ($*p < 0.05$). Results represent means \pm SD from $n = 5$ independent experiments. (B) MIF-mediated AKT kinase activity in Jurkat T cells is attenuated by inhibitors of clathrin-mediated endocytosis. Cells were prepared and treated with rMIF or control buffer and endocytosis inhibitors as under (A). AKT kinase activity was determined by an *in vitro* AKT kinase assay following specific immunoprecipitation (IP) of phosphorylated AKT using a rabbit anti-phospho-AKT antibody. GSK3 α/β was used as the substrate and phosphorylated GSK read-out by Western blot using an anti- α/β rabbit mAb and band densitometry (phosphorylation ratio). The secondary Western blot antibody also detects the rabbit mAb used for the IP (heavy chain). A protein size marker was electrophoresed for comparison (Mr, kDa). The blot shown is representative of two independent AKT kinase assays ($n = 2$).

on MIF-stimulated AKT activation on endocytotic inhibitors was observed in dermal fibroblasts (data not shown), indicating that the differentiation between plasma membrane-associated and endosomal AKT activation upon MIF stimulation may occur in a cell type-specific context.

Discussion

MIF is a potent inflammatory cytokine with chemokine-like activities which plays a pivotal role in acute and chronic inflammatory disease, autoimmunity, and cancer (Calandra and Roger, 2003). MIF target cell action is mediated by the receptors CD74, CXCR2 and CXCR4, which, dependent on their expression profile, may act individually or in concert with each other (Borghese and Clancy, 2011; Noels et al., 2009; Zernecke et al., 2008). As the receptors for MIF have only been discovered relatively recently, the mechanisms of MIF endocytosis have not been well understood. In fact,

initial studies suggested that MIF is predominantly endocytosed by a receptor-independent internalization mechanism (Kleemann et al., 2000, 2002). Closer characterization of the MIF receptor pathways showed that MIF activated the ERK1/2 and/or JNK pathways as well as the PI3K/AKT pathway in a CD74- and/or CXCR4-dependent manner. Both rapid transient and sustained modes of activation have been identified upon MIF stimulation (Coleman et al., 2008; Leng et al., 2003; Lue et al., 2006, 2011). Functional interaction between MIF receptors in MAPK signaling has been best characterized for CD74 and CXCR4 (Lue et al., 2011; Schwartz et al., 2009). Thus, although there is accumulating evidence about MIF signaling via CD74 and CXCR4, knowledge about switch-off mechanisms, often linked to β -arrestin activation and endocytosis of the ligand/receptor complex, has been scarce. Initial evidence in this direction has come from Shi et al. who studied MIF-induced ERK activation using CD74 and CD44 transfectants as well as mutants of these receptor proteins. They uncovered a MIF-triggered serine phosphorylation in the intra-cytoplasmic domain of CD74 that, in a CD44- and protein kinase A (PKA)-dependent manner, led to a decrease in ERK signaling (Shi et al., 2006). Although not addressed in that study, serine phosphorylation of CD74 in the course of MIF signaling may have been the first reported indication of an inactivation of a MIF signaling pathway that may be linked with endocytosis. Xie et al. studied potential connections between MIF-stimulated sustained ERK signaling and endocytosis of MIF in more detail and obtained evidence that the adaptor β -arrestin-1 interacts with CD74 upon MIF stimulation, resulting in MIF endocytosis in a CPZ-sensitive manner and a reduction of sustained ERK signaling. Thus, β -arrestin-1 appears to play a role in coupling MIF endocytosis to sustained ERK activation (Xie et al., 2011). Of note, β -arrestin-1 also is well known for its role in GPCR desensitization, internalization and down-regulation of signal transduction by GPCRs, including CXCR4. However, β -arrestins, which were named for their ability to sterically hinder G protein coupling of agonist-activated GPCRs, resulting in receptor desensitization, can also function to activate signaling cascades independently of G protein activation by serving as scaffolds which bring elements of specific signaling pathways into proximity to each other (DeWire et al., 2007). Whether such mechanisms also apply to MIF-induced CXCR4 activation remains unknown. Also, potential mechanistic links between AKT and JNK signaling, two other prominent pathways activated by MIF, and MIF endocytosis have not been explored.

Here, we have characterized the MIF endocytosis pathway in detail. Applying various endocytotic pathway-specific inhibitors and microscopic colocalization with endosomal markers we show that MIF is internalized by a clathrin-mediated, dynamin-dependent, but caveolin-independent endocytosis pathway. MIF endocytosis is rapid and the pathway is shared with that of LDL and in part with that of transferrin. Importantly, we show that MIF endocytosis is accelerated in the presence of CD74 and is co-dependent on CXCR4. Both receptors could be shown to colocalize with MIF both at the cell membrane and intracellularly in the endosomal pathway. Lastly, our data suggest that MIF-triggered AKT activation is at least in part initiated from endosomal compartments, suggesting that MIF-triggered endosomal signaling can occur.

Our endocytosis studies were performed with Alexa⁵⁴⁶MIF. We took great care that fluorescent labeling of human MIF was performed under native conditions. Labeled MIF exhibited full biological activity and was endotoxin-free. We observed rapid MIF internalization in several cell types. The studied cells include HeLa-type cells, MEFs, HEK293 as well as Jurkat T cells. Internalization of MIF was seen over a wide concentration range, with added MIF at concentrations as low as 30 ng/ml rapidly and efficiently internalized. Xie et al. (2011) and Kleemann et al. (2000) had observed

MIF endocytosis in RAW 264.7 macrophages. Hence, diverse cell types of both immune and non-immune origin are able to endocytose MIF and we suspect that this is coupled to MIF signaling events. MIF rapidly colocalized with endosomal markers and rapid entry of MIF into the endocytic pathway occurred under several experimental conditions. These included addition of Alexa⁵⁴⁶MIF under both physiological (37 °C) and temperature shift conditions (4 °C/37 °C) as well as analysis of fixed cells and live imaging conditions. Colocalization with the late endosomal marker Rab7 was seen as early as 10 min upon MIF addition to cells and could still be detected after up to 160 min.

A closer examination of the endocytotic sub-track followed by MIF (and its receptors) was undertaken by applying the various pathway-specific inhibitors. Although the inhibitory efficiency was not identical for all agents that act through different molecular mechanisms, and also differed between cell types, significant and marked inhibition (up to 62%) of MIF endocytosis was measured and together showed that MIF endocytosis is clathrin- and dynamin-dependent but caveolin-independent. Our results as obtained in fibroblasts, HEK293, and HeLa cells are thus in line with earlier findings by Xie et al. (2011) in RAW264.7 macrophages, who also found that MIF uptake was CPZ-sensitive. Moreover, our study suggests that MIF transport via the endolysosomal compartment requires intact microtubules and a functional acidification of late endosomes via proton pumps, as we observed an appreciable inhibition of MIF trafficking by nocodazole (a microtubule toxin) and bafilomycin (an inhibitor of proton pumps). Intriguingly, blockade with these agents resulted in an arrest of MIF endocytosis and in a consequential swelling of endosome structures. There are known representatives for the different endocytic sub-pathways which are established in mammalian cells. The classical clathrin-mediated endocytosis pathway, which eventually results in the degradation of the internalized ligand in lysosomes is best represented by LDL. In contrast, transferrin internalization which is also clathrin-mediated, is associated with a rapid recycling of the ligand back to the plasma membrane. The uptake of cholera toxin B on the other hand is clathrin-independent and is known to occur through caveolae or lipid raft structures. We found that the MIF endocytosis process was best paralleled by that of LDL. Moreover, MIF colocalized with transferrin early in the endocytotic process but not thereafter, indicating that MIF shares with transferrin early endosomal vesicles, but is not recycled back to the plasma membrane (Dickson et al., 1983; Dunn et al., 1989; Ghosh et al., 1994). Of note, Lakadamyali et al. showed that early endosomes consist of two distinct populations which differ in their maturation time to late endosomes. One population is highly mobile on microtubules and rapidly matures towards late endosomes, whereas the second one is more static with a slow maturation time (Lakadamyali et al., 2006). Our nocodazole blockade results support the notion that MIF traffics through the former population. Very clearly, the cellular uptake of MIF does not follow a caveolin-dependent pathway, as there was neither a colocalization with cholera toxin B nor any significant inhibition of MIF endocytosis by nystatin or filipin.

Several lines of evidence in our study indicate that both CD74 and CXCR4 contribute to MIF endocytosis. Ectopic overexpression of CD74 in HEK293 and HeLa cells, which do not endogenously express CD74, markedly accelerated MIF endocytosis at early time intervals during the endocytotic process with a distinct peak observed at 10–16 min. However, it needs to be emphasized that appreciable MIF endocytosis occurred in the absence of CD74. Because HEK293 and HeLa cells endogenously express medium levels of CXCR4, we suspect that CD74-independent endocytosis of MIF was mediated by CXCR4. Interestingly, Xie et al. did not observe MIF endocytosis in CD74-deficient COS-7 cells. However, COS-7 cells are monkey-derived and are thus deficient for human CXCR4 (Xie et al., 2011). Our confocal microscopy data in HEK293 cells

showing prominent colocalization between Alexa⁵⁴⁶MIF and transiently expressed YFP-CD74 and CFP-CXCR4 after 30 min of MIF addition support a role for CXCR4 in MIF endocytosis. This notion was further underscored by the AMD3100 experiments, a CXCR4-specific inhibitor, which led to a 40% reduction of colocalization between MIF and Rab7GFP. Coordinate action of CD74 and CXCR4 in MIF-stimulated AKT and JNK signaling in Jurkat T cells (Lue et al., 2011; Schwartz et al., 2009) additionally indicates that these receptors may also play a role in MIF endocytosis. In fact, when we studied MIF-driven AKT responses in the presence of endocytosis inhibitors such as CPZ, we noted a reduction of phosphorylated AKT and of AKT kinase activity when compared to DMSO-treated control incubations. This effect was marked and significant in Jurkat cells which express both CD74 and CXCR4 while it showed a trend in HeLa cells which only express CXCR4 but not CD74. Together, this suggested that MIF-mediated AKT signaling is at least in part due to endosomal signaling and likely relies on functional CD74/CXCR4 complexes (Schwartz et al., 2009). Lack of significant MIF-mediated AKT signaling in non-transfected HeLa could also indicate that CXCR4 skews the MIF/AKT signaling response towards a plasma membrane phenotype, while CD74 may promote endosomal signaling. The observation that MIF-mediated AKT signaling was not blockable by CPZ in human dermal fibroblasts, which express both CD74 and CXCR4 at low-medium level indicated that the distribution of plasma membrane-borne versus endosome-derived MIF signaling additionally is cell-dependent.

CD74 is known to undergo recycling of plasma membrane passages with a half-life of about 3–4 min at the cell surface (Henne et al., 1995). CD74 is a type II transmembrane glycoprotein associated with MHC class II molecules and is hence a good candidate to mediate AKT activation via endosomal signaling because it is known to target human leukocyte antigen (HLA)-DR molecules to subcellular endocytic compartments and to be processed in endocytic compartments. In fact, in a MHC class II-positive cell type CD74 is expressed in the endolysosomal compartment to a large part. Moldenhauer and coworkers could even illustrate colocalization between HLA-DR-complexed CD74 and early endosomes. Furthermore, they demonstrated that CD74, which first associates with MHC class II α and β chains in the lumen of the ER, initiates the transport of class II molecules to late endosomes and lysosomes (Moldenhauer et al., 1999). To identify the proteins which sequester CD74 to the endosomal compartment in the absence of MHC class II will merit future attention.

A direct interaction with β -arrestin was shown for both CD74 and CXCR4 (Lagane et al., 2008; Xie et al., 2011). More recently, it has been recognized that β -arrestins, beyond their ability to act as negative regulators of GPCRs and other receptors, can also function as scaffold proteins for SRC family members and can promote receptor signaling after endocytosis. The SHSK motif in the third intracellular loop of CXCR4 was identified as a direct interaction site between CXCR4 and β -arrestin (Cheng et al., 2000). While β -arrestin binding to the C-terminal tail of a chemokine receptor elicits internalization and desensitization, interaction with the intracellular loops supports β -arrestin-mediated signaling (Borroni et al., 2010). The exact β -arrestin binding motif for CD74 remains unknown, although a LxxxPML motif is located in the cytoplasmic sequence of CD74 which serves as a recognition motif for the clathrin adaptors AP1 and AP2 (Hofmann et al., 1999).

The CXCR4 internalization pathway is fairly well understood. CXCR4 follows a clathrin-mediated endocytic pathway (Signoret et al., 1997) and can internalize both constitutively and in a ligand-induced manner (Futahashi et al., 2007). CXCR4 sorting to lysosomes is Rab7-dependent and can be promoted by prolonged exposure to its ligands (Marchese et al., 2008; Zhang et al., 2004). Thus, current knowledge about the endocytosis mechanisms of CD74 and CXCR4 is well in line with the endocytic mechanism

identified for MIF in our study. Likewise, although for many chemokine receptors an inhibition of endocytosis correlates with a lack of signaling activation, internalization-dead CXCR4 mutants still signal and interact with β -arrestin. The residual MIF-induced AKT activation in CD74-negative and CPZ-treated cells could therefore be mediated through CXCR4 plasma membrane signaling. Future mechanistic studies will need to address which factors are involved in MIF-driven AKT activation and how this correlates with MIF endocytosis. Candidate proteins could be β -arrestin-1, AP-2, annexin-8, myosin II A and other factors.

As herein, we have characterized the MIF endocytosis pathway to be rapid, clathrin- and dynamin-dependent, microtubule- and acidification-driven, LDL-like, and dependent on CD74 and CXCR4, such future analyses should be greatly facilitated.

Acknowledgements

We thank B. Lennartz for the preparation of recombinant MIF and G. Müller-Newen and his LSM team for invaluable advice with the confocal microscopy technology and the LSM instruments. We thank L. Leng and R. Bucala for the pcDNA3.1/V5-His-TOPO-CD74 plasmid. This work was supported by grants from the Deutsche Forschungsgemeinschaft (DFG) to J.B., T.O., and C.W. (DFG-SFB542 project A7 and DFG-FOR809 project Be1977/4-2).

Appendix A. Supplementary data

Supplementary data associated with this article can be found, in the online version, at [doi:10.1016/j.ejcb.2011.08.006](https://doi.org/10.1016/j.ejcb.2011.08.006).

References

- Berndt, K., Kim, M., Meinhardt, A., Klug, J., 2008. Macrophage migration inhibitory factor does not modulate co-activation of androgen receptor by Jab1/CNS5. *Mol. Cell. Biochem.* 307, 265–271.
- Bernhagen, J., Krohn, R., Lue, H., Gregory, J.L., Zerneck, A., Koenen, R.R., Dewor, M., Georgiev, I., Schober, A., Leng, L., Kooistra, T., Fingerle-Rowson, G., Ghezzi, P., Kleemann, R., McColl, S.R., Bucala, R., Hickey, M.J., Weber, C., 2007. MIF is a noncognate ligand of CXCR4 chemokine receptors in inflammatory and atherogenic cell recruitment. *Nat. Med.* 13, 587–596.
- Bernhagen, J., Mitchell, R.A., Calandra, T., Voelter, W., Cerami, A., Bucala, R., 1994. Purification, bioactivity, and secondary structure analysis of mouse and human macrophage migration inhibitory factor (MIF). *Biochemistry* 33, 14144–14155.
- Binsky, I., Haran, M., Starlets, D., Gore, Y., Lantner, F., Harpaz, N., Leng, L., Goldenberg, D.M., Shvidel, L., Berrebi, A., Bucala, R., Shachar, I., 2007. IL-8 secreted in a macrophage migration-inhibitory factor- and CD74-dependent manner regulates B cell chronic lymphocytic leukemia survival. *Proc. Natl. Acad. Sci. U.S.A.* 104, 13408–13413.
- Borghese, F., Clanchy, F.L., 2011. CD74: an emerging opportunity as a therapeutic target in cancer and autoimmune disease. *Expert Opin. Ther. Targets* 15, 237–251.
- Borroni, E.M., Mantovani, A., Locati, M., Bonecchi, R., 2010. Chemokine receptors intracellular trafficking. *Pharmacol Ther* 127, 1–8.
- Burger-Kentscher, A., Goebel, H., Seiler, R., Fraedrich, G., Schaefer, H.E., Dimmeler, S., Kleemann, R., Bernhagen, J., Ihling, C., 2002. Expression of macrophage migration inhibitory factor in different stages of human atherosclerosis. *Circulation* 105, 1561–1566.
- Busch, R., Rinderknecht, C.H., Roh, S., Lee, A.W., Harding, J.J., Burster, T., Hornell, T.M., Mellins, E.D., 2005. Achieving stability through editing and chaperoning: regulation of MHC class II peptide binding and expression. *Immunol. Rev.* 207, 242–260.
- Calandra, T., Roger, T., 2003. Macrophage migration inhibitory factor: a regulator of innate immunity. *Nat. Rev. Immunol.* 3, 791–800.
- Carpenter, G., Cohen, S., 1979. Epidermal growth factor. *Annu. Rev. Biochem.* 48, 193–216.
- Cheng, Z.J., Zhao, J., Sun, Y., Hu, W., Wu, Y.L., Cen, B., Wu, G.X., Pei, G., 2000. Beta-arrestin differentially regulates the chemokine receptor CXCR4-mediated signaling and receptor internalization, and this implicates multiple interaction sites between beta-arrestin and CXCR4. *J. Biol. Chem.* 275, 2479–2485.
- Cho, Y., Crichlow, G.V., Vermeire, J.J., Leng, L., Du, X., Hodsdon, M.E., Bucala, R., Cappello, M., Gross, M., Gaeta, F., Johnson, K., Lolis, E.J., 2010. Allosteric inhibition of macrophage migration inhibitory factor revealed by ibudilast. *Proc. Natl. Acad. Sci. U.S.A.* 107, 11313–11318.
- Coleman, A.M., Rendon, B.E., Zhao, M., Qian, M.W., Bucala, R., Xin, D., Mitchell, R.A., 2008. Cooperative regulation of non-small cell lung carcinoma angiogenic potential by macrophage migration inhibitory factor and its homolog, D-dopachrome tautomerase. *J. Immunol.* 181, 2330–2337.
- Damke, H., Baba, T., Warnock, D.E., Schmid, S.L., 1994. Induction of mutant dynamin specifically blocks endocytic coated vesicle formation. *J. Cell Biol.* 127, 915–934.
- Desseine, A.F., Stechly, L., Jonckheere, N., Dumont, P., Monte, D., Leteurtre, E., Truant, S., Pruvot, F.R., Figeac, M., Hebbard, M., Lecellier, C.H., Lesuffeur, T., Desseine, R., Grard, G., Dejonghe, M.J., de Launoit, Y., Furuichi, Y., Prevost, G., Porchet, N., Gespach, C., Huet, G., 2010. Autocrine induction of invasive and metastatic phenotypes by the MIF-CXCR4 axis in drug-resistant human colon cancer cells. *Cancer Res.* 70, 4644–4654.
- DeWire, S.M., Ahn, S., Lefkowitz, R.J., Shenoy, S.K., 2007. Beta-arrestins and cell signaling. *Annu. Rev. Physiol.* 69, 483–510.
- Dickson, R.B., Hanover, J.A., Willingham, M.C., Pastan, I., 1983. Prelysosomal divergence of transferrin and epidermal growth factor during receptor-mediated endocytosis. *Biochemistry* 22, 5667–5674.
- Dunn, K.W., McGraw, T.E., Maxfield, F.R., 1989. Iterative fractionation of recycling receptors from lysosomally destined ligands in an early sorting endosome. *J. Cell Biol.* 109, 3303–3314.
- Futahashi, Y., Komano, J., Urano, E., Aoki, T., Hamatake, M., Miyauchi, K., Yoshida, T., Koyanagi, Y., Matsuda, Z., Yamamoto, N., 2007. Separate elements are required for ligand-dependent and -independent internalization of metastatic potential CXCR4. *Cancer Sci* 98, 373–379.
- Ghosh, R.N., Gelman, D.L., Maxfield, F.R., 1994. Quantification of low density lipoprotein and transferrin endocytic sorting Hep2 cells using confocal microscopy. *J. Cell Sci.* 107 (Pt 8), 2177–2189.
- Goldstein, J.L., Anderson, R.G., Brown, M.S., 1979. Coated pits, coated vesicles, and receptor-mediated endocytosis. *Nature* 279, 679–685.
- Goldstein, J.L., Brown, M.S., Anderson, R.G., Russell, D.W., Schneider, W.J., 1985. Receptor-mediated endocytosis: concepts emerging from the LDL receptor system. *Annu. Rev. Cell Biol.* 1, 1–39.
- Gould, G.W., Lippincott-Schwartz, J., 2009. New roles for endosomes: from vesicular carriers to multi-purpose platforms. *Nat. Rev. Mol. Cell Biol.* 10, 287–292.
- Henne, C., Schwenk, F., Koch, N., Moller, P., 1995. Surface expression of the invariant chain (CD74) is independent of concomitant expression of major histocompatibility complex class II antigens. *Immunology* 84, 177–182.
- Hofmann, M.W., Honing, S., Rodionov, D., Dobberstein, B., von Figura, K., Bakke, O., 1999. The leucine-based sorting motifs in the cytoplasmic domain of the invariant chain are recognized by the clathrin adaptors AP1 and AP2 and their medium chains. *J. Biol. Chem.* 274, 36153–36158.
- Kleemann, R., Grell, M., Mischke, R., Zimmermann, G., Bernhagen, J., 2002. Receptor binding and cellular uptake studies of macrophage migration inhibitory factor (MIF): use of biologically active labeled MIF derivatives. *J. Interferon Cytokine Res.* 22, 351–363.
- Kleemann, R., Hauser, A., Geiger, G., Mischke, R., Burger-Kentscher, A., Flieger, O., Johannes, F.J., Roger, T., Calandra, T., Kapurniotu, A., Grell, M., Finkelmeier, D., Brunner, H., Bernhagen, J., 2000. Intracellular action of the cytokine MIF to modulate AP-1 activity and the cell cycle through Jab1. *Nature* 408, 211–216.
- Lagane, B., Chow, K.Y., Balabanian, K., Levoe, A., Harriague, J., Planchenault, T., Baleux, F., Gunera-Saad, N., Arenzana-Seisdedos, F., Bachelier, F., 2008. CXCR4 dimerization and beta-arrestin-mediated signaling account for the enhanced chemotaxis to CXCL12 in WHIM syndrome. *Blood* 112, 34–44.
- Lakadamyali, M., Rust, M.J., Zhuang, X., 2006. Ligands for clathrin-mediated endocytosis are differentially sorted into distinct populations of early endosomes. *Cell* 124, 997–1009.
- Leng, L., Metz, C.N., Fang, Y., Xu, J., Donnelly, S., Baugh, J., Delohery, T., Chen, Y., Mitchell, R.A., Bucala, R., 2003. MIF signal transduction initiated by binding to CD74. *J. Exp. Med.* 197, 1467–1476.
- Lue, H., Dewor, M., Leng, L., Bucala, R., Bernhagen, J., 2011. Activation of the JNK signalling pathway by macrophage migration inhibitory factor (MIF) and dependence on CXCR4 and CD74. *Cell. Signal.* 23, 135–144.
- Lue, H., Kapurniotu, A., Fingerle-Rowson, G., Roger, T., Leng, L., Thiele, M., Calandra, T., Bucala, R., Bernhagen, J., 2006. Rapid and transient activation of the ERK MAPK signalling pathway by macrophage migration inhibitory factor (MIF) and dependence on JAB1/CNS5 and Src kinase activity. *Cell. Signal.* 18, 688–703.
- Lue, H., Thiele, M., Franz, J., Dahl, E., Speckgens, S., Leng, L., Fingerle-Rowson, G., Bucala, R., Luscher, B., Bernhagen, J., 2007. Macrophage migration inhibitory factor (MIF) promotes cell survival by activation of the Akt pathway and role for CNS5/JAB1 in the control of autocrine MIF activity. *Oncogene* 26, 5046–5059.
- Marchese, A., Chen, C., Kim, Y.M., Benovic, J.L., 2003. The ins and outs of G protein-coupled receptor trafficking. *Trends Biochem. Sci.* 28, 369–376.
- Marchese, A., Paing, M.M., Temple, B.R., Trejo, J., 2008. G protein-coupled receptor sorting to endosomes and lysosomes. *Annu. Rev. Pharmacol. Toxicol.* 48, 601–629.
- Matza, D., Kerem, A., Shachar, I., 2003. Invariant chain, a chain of command. *Trends Immunol.* 24, 264–268.
- Meyer-Siegler, K.L., Iczkowski, K.A., Leng, L., Bucala, R., Vera, P.L., 2006. Inhibition of macrophage migration inhibitory factor or its receptor (CD74) attenuates growth and invasion of DU-145 prostate cancer cells. *J. Immunol.* 177, 8730–8739.
- Miaczynska, M., Bar-Sagi, D., 2010. Signaling endosomes: seeing is believing. *Curr. Opin. Cell Biol.* 22, 535–540.
- Miaczynska, M., Pelkmans, L., Zerial, M., 2004. Not just a sink: endosomes in control of signal transduction. *Curr. Opin. Cell Biol.* 16, 400–406.
- Moldenhauer, G., Henne, C., Karhausen, J., Moller, P., 1999. Surface-expressed invariant chain (CD74) is required for internalization of human leucocyte antigen-DR molecules to early endosomal compartments. *Immunology* 96, 473–484.

- Montesano, R., Roth, J., Robert, A., Orci, L., 1982. Non-coated membrane invaginations are involved in binding and internalization of cholera and tetanus toxins. *Nature* 296, 651–653.
- Moser, B., Loetscher, P., 2001. Lymphocyte traffic control by chemokines. *Nat. Immunol.* 2, 123–128.
- Murphy, P.M., Baggiolini, M., Charo, I.F., Hebert, C.A., Horuk, R., Matsushima, K., Miller, L.H., Oppenheim, J.J., Power, C.A., 2000. International union of pharmacology. XXII. Nomenclature for chemokine receptors. *Pharmacol. Rev.* 52, 145–176.
- Nguyen, M.T., Lue, H., Kleemann, R., Thiele, M., Tolle, G., Finkelmeier, D., Wagner, E., Braun, A., Bernhagen, J., 2003. The cytokine macrophage migration inhibitory factor reduces pro-oxidative stress-induced apoptosis. *J. Immunol.* 170, 3337–3347.
- Noels, H., Bernhagen, J., Weber, C., 2009. Macrophage migration inhibitory factor: a noncanonical chemokine important in atherosclerosis. *Trends Cardiovasc. Med.* 19, 76–86.
- Rot, A., von Andrian, U.H., 2004. Chemokines in innate and adaptive host defense: basic chemokine grammar for immune cells. *Annu. Rev. Immunol.* 22, 891–928.
- Schober, A., Bernhagen, J., Thiele, M., Zeffer, U., Knarren, S., Roller, M., Bucala, R., Weber, C., 2004. Stabilization of atherosclerotic plaques by blockade of macrophage migration inhibitory factor after vascular injury in apolipoprotein E-deficient mice. *Circulation* 109, 380–385.
- Schwartz, V., Lue, H., Kraemer, S., Korbiel, J., Krohn, R., Ohl, K., Bucala, R., Weber, C., Bernhagen, J., 2009. A functional heteromeric MIF receptor formed by CD74 and CXCR4. *FEBS Lett.* 583, 2749–2757.
- Shi, X., Leng, L., Wang, T., Wang, W., Du, X., Li, J., McDonald, C., Chen, Z., Murphy, J.W., Lolis, E., Noble, P., Knudson, W., Bucala, R., 2006. CD44 is the signaling component of the macrophage migration inhibitory factor-CD74 receptor complex. *Immunity* 25, 595–606.
- Signoret, N., Oldridge, J., Pelchen-Matthews, A., Klasse, P.J., Tran, T., Brass, L.F., Rosenkilde, M.M., Schwartz, T.W., Holmes, W., Dallas, W., Luther, M.A., Wells, T.N., Hoxie, J.A., Marsh, M., 1997. Phorbol esters and SDF-1 induce rapid endocytosis and down modulation of the chemokine receptor CXCR4. *J. Cell Biol.* 139, 651–664.
- Simons, D., Grieb, G., Hristov, M., Pallua, N., Weber, C., Bernhagen, J., Steffens, G., 2011. Hypoxia-induced endothelial secretion of macrophage migration inhibitory factor and role in endothelial progenitor cell recruitment. *J. Cell. Mol. Med.* 15, 668–678.
- Son, A., Kato, N., Horibe, T., Matsuo, Y., Mochizuki, M., Mitsui, A., Kawakami, K., Nakamura, H., Yodoi, J., 2009. Direct association of thioredoxin-1 (TRX) with macrophage migration inhibitory factor (MIF): regulatory role of TRX on MIF internalization and signaling. *Antioxid. Redox Signal.* 11, 2595–2605.
- Sorkin, A., von Zastrow, M., 2002. Signal transduction and endocytosis: close encounters of many kinds. *Nat. Rev. Mol. Cell Biol.* 3, 600–614.
- Stern, L.J., Potoicchio, I., Santambrogio, L., 2006. MHC class II compartment subtypes: structure and function. *Curr. Opin. Immunol.* 18, 64–69.
- Tarnowski, M., Grymula, K., Liu, R., Tarnowska, J., Drukala, J., Ratajczak, J., Mitchell, R.A., Ratajczak, M.Z., Kucia, M., 2010. Macrophage migration inhibitory factor is secreted by rhabdomyosarcoma cells, modulates tumor metastasis by binding to CXCR4 and CXCR7 receptors and inhibits recruitment of cancer-associated fibroblasts. *Mol. Cancer Res.* 8, 1328–1343.
- Thelen, M., Stein, J.V., 2008. How chemokines invite leukocytes to dance. *Nat. Immunol.* 9, 953–959.
- Thomson, A.W., 2003. *The Cytokine Handbook*. Academic Press, New York, NY, USA.
- Tran, D., Carpentier, J.L., Sawano, F., Gorden, P., Orci, L., 1987. Ligands internalized through coated or noncoated invaginations follow a common intracellular pathway. *Proc. Natl. Acad. Sci. U.S.A.* 84, 7957–7961.
- Vera, P.L., Iczkowski, K.A., Wang, X., Meyer-Siegler, K.L., 2008. Cyclophosphamide-induced cystitis increases bladder CXCR4 expression and CXCR4-macrophage migration inhibitory factor association. *PLoS ONE* 3, e3898.
- von Zastrow, M., Sorkin, A., 2007. Signaling on the endocytic pathway. *Curr. Opin. Cell Biol.* 19, 436–445.
- Wall, D.A., Wilson, G., Hubbard, A.L., 1980. The galactose-specific recognition system of mammalian liver: the route of ligand internalization in rat hepatocytes. *Cell* 21, 79–93.
- Weber, C., Schober, A., Zerneck, A., 2004. Chemokines: key regulators of mononuclear cell recruitment in atherosclerotic vascular disease. *Arterioscler. Thromb. Vasc. Biol.* 24, 1997–2008.
- Xie, L., Qiao, X., Wu, Y., Tang, J., 2011. beta-Arrestin1 mediates the endocytosis and functions of macrophage migration inhibitory factor. *PLoS ONE* 6, e16428.
- Zerneck, A., Bernhagen, J., Weber, C., 2008. Macrophage migration inhibitory factor in cardiovascular disease. *Circulation* 117, 1594–1602.
- Zhang, Y., Foudi, A., Geay, J.F., Berthebaud, M., Buet, D., Jarrier, P., Jalil, A., Vainchenker, W., Louache, F., 2004. Intracellular localization and constitutive endocytosis of CXCR4 in human CD34+ hematopoietic progenitor cells. *Stem Cells* 22, 1015–1029.